JOURNAL OF GEOPHYSICAL RESEARCH, VOL. 97, NO. B13, PAGES 19,929–19,947, DECEMBER 10, 1992

Attenuation of High-Frequency Seismic Waves Beneath the Central Andean Plateau

DEAN WHITMAN[1], BRYAN L. ISACKS[1], JEAN-LUC CHATELAIN[2], JER-MING CHIU[3], AND ALEJANDRO PEREZ[4]

Observed patterns of high-frequency seismic wave attenuation suggest that near 22° S, the upper mantle structure beneath the central Andean plateau changes along strike to the south. Contrasting regions of high and low upper mantle seismic wave attenuation beneath the plateau are identified based on striking azimuthal variations in the character and frequency content of *P* and *S* waves propagating beneath the plateau to a portable seismic network deployed in Jujuy Province, Argentina (24° S, 65° W). Ray paths from intermediate depth earthquakes located north and northwest of the network transmit seismic waves with a higher frequency content than ray paths from earthquakes at similar depths and distances but located west and south of the network. The estimated apparent *Q* values fall into two categories: $Qp > 500$ and $Qs > 350$ for the high-*Q* paths, and $Qp < 350$ and $Qs < 200$ for the low-*Q* paths. In addition, *Sn* phases from regional crustal earthquakes in the Subandean foreland fold-thrust belt to the north propagate efficiently to the Jujuy network, while *Sn* is not observed from foreland earthquakes located at similar distances to the south of the network. These observations combined with data from previously reported wave propagation studies suggest that south of about 22° S, the upper mantle beneath the plateau and its adjacent foreland thrust belt is more highly attenuating than the upper mantle farther north. Forward modeling of the *Q* measurements made at Jujuy indicates that the observations can be explained either by a variable thickness high-*Q* upper plate beneath the plateau, or by a thin, variable width, very low-*Q* zone in the asthenospheric wedge above the subducted slab. This lateral variation in upper mantle structure coincides with two physiographically distinct segments of the central Andean plateau and its adjacent foreland thrust belt to the east: the Bolivian Altiplano and Subandean ranges in the north and the Argentine Puna and Santa Barbara system in the south. We interpret the north-south change in upper mantle attenuation and the corresponding changes in physiography, topography, and tectonic style at the surface to be due to a mantle lid that is thicker beneath the Altiplano and the Subandean belt than beneath the Puna and the Santa Barbara ranges.

INTRODUCTION

The central Andean plateau, comprising the Peruvian and Bolivian Altiplano and the Argentine Puna, occupies a region about 300 km wide and 2000 km long with an average elevation near 4 km [*Isacks*, 1988] (Figure 1). The Altiplano-Puna is rivaled on land in areal extent and average elevation only by the Tibetan plateau. While the uplift of the Tibetan plateau is clearly related to the convergence of buoyant continental plates, the central Andean plateau occurs adjacent to an oceanic-continental convergence zone where the oceanic Nazca plate is being subducted beneath South American plate. In both regions the mechanisms to account for the plateau uplift remain controversial. Proposed mechanisms of Andean uplift include magmatic additions to the crust [e.g., *Thorpe et al.*, 1981], crustal shortening [*Jordan et al.*, 1983; *Lyon-Caen et al.*, 1985; *Roeder*, 1988; *Sheffels*, 1990], or some combination of compressional crustal shortening and thickening, and lithospheric thinning and thermal expansion [*Froidevaux and Isacks*, 1984; *Isacks* 1988].

A knowledge of the crustal and upper mantle structure beneath the plateau provides important constraints on various thermal and mechanical models for uplift of the plateau. The existence of a thick lithospheric lid implies that the topography of the plateau is compensated mainly by crustal thickening, whereas a thin lid implies that a significant component of the plateau's elevation is supported by thermal thinning of the lithosphere. One of the most sensitive indicators of upper mantle lid structure is the efficiency of high-frequency *P* and *S* wave propagation from sources at regional distances. High-frequency seismic waves that pass through the asthenosphere are more strongly attenuated than those with paths confined solely to the lithosphere. In general, efficient high-frequency wave propagation is observed within shields and stable continental regions whereas inefficient wave propagation is observed within areas of thinned or discontinuous lithosphere and behind volcanic arcs. [e.g., *Molnar and Oliver*, 1969; *Barazangi and Isacks*, 1971]. Previously, some studies have found that the upper mantle beneath the Altiplano-Puna is a zone of anomalously high seismic wave attenuation suggesting a thin lithosphere beneath the plateau [*Molnar and Oliver*, 1969; *Barazangi et al.*, 1975; *Chinn et al.*, 1980], while other studies have suggested that the plateau is underlain by a relatively thick continental lithosphere of at least 150 km with high seismic wave attenuation confined to a thin zone directly above the surface of the subducted slab [*James*, 1971a; *Sacks*, 1971; *Sacks and Okada*, 1974]. This study attempts to resolve some of the discrepancies between these previous studies.

In this study, we map lateral variations in upper mantle *P* and *S* wave attenuation beneath the plateau using observations of seismic waveforms from shallow and intermediate depth earthquakes recorded by a portable seismic array deployed in

[1]Institute for the Study of the Continents (INST)C and Department of Geological Sciences,cornell University, Ithaca, New York.

[2]Office de la Recherche Scientifique et Technique Outre-Mer (ORSTOM), IRIGM-LGIT, Universite J. Fourier, Grenoble, France.

[3]Center for Earthquake Research and Information, Memphis State University, Memphis, Tennessee.

[4]Instituto de Minería y Geología, Universidad Nacionál de Jujuy, S. S. de Jujuy, Argentina.

Paper number 92JB01748.
0148-0227/92/92JB-01748$05.00

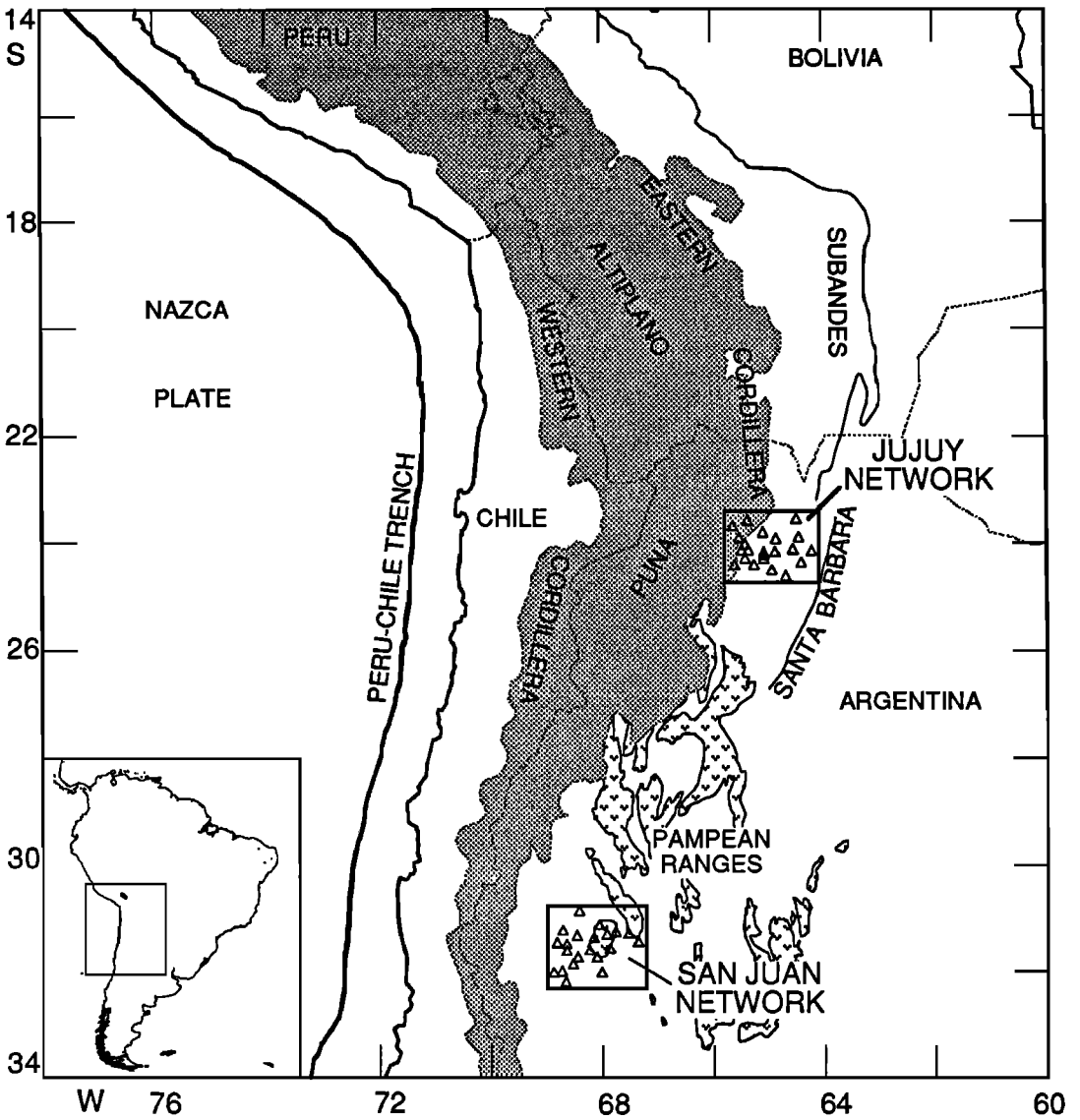

Fig. 1. Map showing location of the PANDA deployments with respect to major tectonic and physiographic features of the central Andes. The shaded area on the map represents regions with over 3-km average elevation.

Jujuy Province, Argentina. Large differences in the amplitudes and frequencies of *P* and *S* waves recorded from earthquakes at various azimuths, depths, and distances indicate substantial variations in the upper mantle attenuation structure beneath the Altiplano-Puna plateau and its adjacent foreland. *Q* measurments made at the Jujuy network are modeled to explore the possible range of upper mantle structure required to explain the observations. The new data can be combined with the extensive mapping of seismic wave propagation of *Chinn et al.* [1980] to resolve regional scale systematic differences in upper mantle attenuation beneath the Altiplano of Bolivia compared with the Argentine Puna. These differences can be correlated with along-strike differences in the physiography and average elevation of the plateau, with differences in the distribution of recent volcanics in the main arc and back arc, and with the styles of foreland deformation along the eastern margins of the plateau. These correlations are interpreted to be due to along-strike changes in lithospheric thickness beneath the plateau.

Tectonic Setting

The margin of western South America is often used as a typical example of an orogen caused by subduction of an oceanic plate beneath a continent [e.g., *Dewey and Bird*, 1970; *James*, 1971b]. This "Andean" style margin is characterized by an active magmatic arc flanked by a trench to the west and a compressional "foreland" fold-thrust system to the east. Numerous authors have noted the relationship between the shape of the subducted Nazca plate and along strike changes in tectonic style of the central Andes (Figure 1) [*Barazangi and Isacks*, 1976; *Pilger*, 1981; *Jordan et al.* 1983; *Isacks*, 1988]. Above regions where the subducted slab dips eastward at around 30°, the Andes are characterized from west to east by an active volcanic arc in the Western Cordillera, a broad high plateau, and an active thin-skinned foreland fold-thrust belt. South of 27°S, above a region of nearly horizontal subduction, recent volcanism is absent, the high mountain belt is much narrower and the foreland structure of the Pampean ranges is dominated

by thick-skinned Laramide style basement uplifts on steeply east and west dipping reverse faults.

We focus on an area between 17°S and 28°S above the 30° dipping segment the subducted Nazca plate: the central Andean plateau and its adjacent foreland to the east. In this region, the plateau can be subdivided into two distinct physiographic provinces. The boundary between these provinces occurs near 22° S, and is approximately coincident with the Argentine-Bolivian border. The northern segment, the Altiplano of southern Peru and Bolivia, is characterized by a single, internally drained and low relief basin trending N-NW between the main volcanic arc on the west and the Miocene volcanic rocks and thrust belt of the Eastern Cordillera. In contrast to the Altiplano, the Puna of northwestern Argentina is characterized by smaller and more fragmented basins, more extensive volcanism, and greater structural relief [*Baker*, 1981; *Jordan and Alonso*, 1987; *Fielding*, 1989].

The foreland fold-thrust belts to the east of the Altiplano and Puna also exhibit differing tectonic styles. Located east of the Altiplano, the Subandean belt is characterized by eastward verging thin-skinned folding and thrusting. Predominantly west-dipping thrusts in an eastward tapering Paleozoic and younger sedimentary wedge are inferred to sole into a basal decollement at depth with deformation confined to the overlying sedimentary package [*Mingramm et al.*, 1979; *Roeder*, 1988; *Baby et al.*, 1989; *Sheffels*, 1990]. In contrast, the foreland fold-thrust belt to the east of the Puna, the Santa Barbara system, is characterized by high-angle, east and west dipping reverse faults which expose Mesozoic and older strata, and which exhibit a greater degree of basement involvement than the Subandean thrusts to the north [*Mingramm et al.*, 1979; *Allmendinger et al.*, 1983; *Jordan et al.* 1983; *Cahill et al.*, 1992].

Recent work has emphasized the importance of paleogeology on the tectonic style in the forelands [*Allmendinger et al.*, 1983; *Grier*, 1990; *Cahill et al.*, 1992]. North of 24° S, the thin-skinned Subandean thrust belt is confined to a thick, eastward tapering, Paleozoic sedimentary wedge which controls the geometry of the thrust belt. In the Santa Barbara system to the south, high-angle reverse faulting and folding appears to be controlled by the location of Cretaceous extensional basins. This would suggest that the style of deformation is controlled by preexisting structures in the crust. However, a primary result of this study is that the surface geological and morphological differences between the Altiplano and the Puna and their adjacent forelands are coincident with differing upper mantle structures beneath each segment. We conclude that mantle structure and consequent rheological differences of the foreland lithosphere may also play an important role in the the variations in the style of foreland deformation.

SEISMIC DATA

The data used for this study consist of digital seismograms from regional earthquakes which were recorded during two separate deployments of a portable seismic network on the eastern margin of the Andes in western Argentina (Figures 1 and 2). In late 1987, 40 seismic stations of the Memphis State University PANDA network were deployed in the Pampean ranges and frontal cordillera of San Juan Province, Argentina. After one year of operation, the network was moved 800 km north and deployed within the basins and ranges of the Eastern Cordillera and Santa Barbara system in and around the province of Jujuy in northwest Argentina. This study primarily employs data collected from regional earthquakes recorded during the 9-month Jujuy deployment. Data collected during the San Juan deployment is shown only for comparison.

Each PANDA instrument [*Chiu et al.*, 1991] is a portable seismograph equipped with two 4.5-Hz three-component seismometers connected to high- and low-gain amplifiers. Station locations were determined from a global positioning system (GPS), which provided station elevations and geographic coordinates to within 10 m accuracy. The data were telemetered via several FM radio links to a central recording location and digitized by the field computer at a rate of 100 samples per second. Common timing among stations was provided by a satellite clock connected to the field computer. Details of the San Juan and Jujuy deployments and data acquisition are given in *Smalley et al.* [1992] and *Cahill et al.* [1992].

Seismic sources used in this study include 98 intermediate depth earthquakes located to the west, northwest, and southwest of the Jujuy network within the subducted Nazca plate, one deep focus earthquake located southeast of the network, and seven crustal earthquakes located within the Andean forelands to the north and south of the network (Figure 2). Earthquake locations are taken from the U.S. Geological Survey Preliminary Determination of Epicenters (PDE) and the International Seismological Centre (ISC). The network data alone permitted clear discrimination between crustal and intermediate depth earthquakes on the basis of a visual examination of the data, analysis of *S-P* times, and measured slowness across the array. In cases where the reported depths were clearly wrong, (e.g., events which from our network data were intermediate depth events but which had reported depths constrained to 33 km), we revised the location by supplementing the reported phase times in the ISC catalogue with *P* and *S* arrival times at the Jujuy network. In one case, arrival times at the network alone were used to locate the hypocenter. In general, the hypocentral backazimuths predicted from the reported locations are in close agreement to those predicted by travel time slowness measurements across the network. The relatively large distance of most of the events to the Jujuy network make the reported hypocenters accurate enough for the purpose of this study.

The appearance and frequency content of *P* and *S* waves observed at Jujuy vary greatly depending on the distance and azimuth to the source. These variations are most clearly manifested in the *S* waves, but similar relationships are also observed for the *P* waves. We have identified three basic types of shear waves: (1) well-defined shear waves with predominant frequencies of 3-4 Hz, (2) those with frequencies around 1 Hz, and (3) waves of an indeterminant nature with absent or poorly defined shear waves and a highly scattered character (Figures. 3 and 4). Fourier amplitude spectra of two shear waves representative of high- and low-Q paths from two intermediate depth earthquakes are shown in Figure 4. The high-frequency *S* waves contain energy with frequencies up to 4 Hz, while the low-frequency *S* waves contain no energy with frequencies greater than 2 Hz. The observed differences in frequency content are not subtle and are clearly resolvable in spite of the rather limited bandwidth of the data. In the next section, we will show that they are not likely due to systematic differences in the seismic source spectra. Instead, we infer the high- and low-frequency seismic waves to be representative of differing amounts of seismic wave attenuation along their respective ray paths.

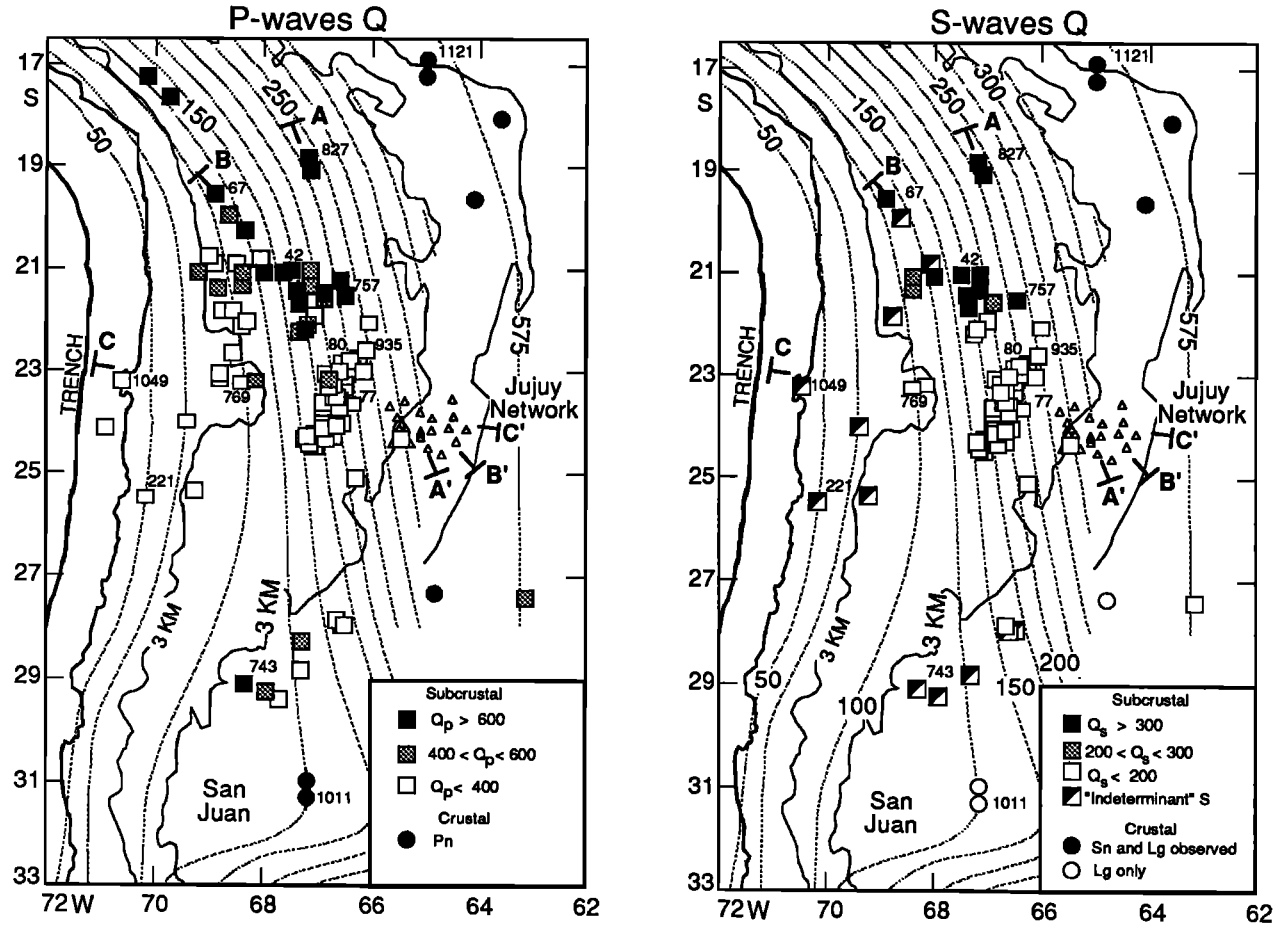

Fig. 2. Estimated apparent Q for P (left) and S (right) wave ray paths to the Jujuy network. Map shows shape of the subducted Nazca plate (labeled contours) [after *Cahill*, 1990, *Cahill and Isacks*, 1992], 3-km average elevation contour, and locations of earthquakes used in the attenuation study. Earthquake locations are from the PDE and ISC. Numbered earthquakes are events referred to in the subsequent figures. Note that events producing high-Q ray paths (dark shaded circles and squares) are all located to the north and northwest of the Jujuy network (small triangles).

ESTIMATION OF Q

In order to gain a more quantitative knowledge of the seismic wave attenuation, average apparent Q for each event was estimated from the spectral decay of the observed P and S waves. Assuming a frequency independent Q, the amplitude spectrum of a wave arriving at a path integrated travel time, t, is

$$A(f) = S(f)\, R(f)\, I(f)\, e^{-\pi t f/Q}$$

where $S(f)$ is the source spectrum, $R(f)$ is the receiver site response spectrum, and $I(f)$ is the instrument system response. In general, only $I(f)$ is well known and $S(f)$ and $R(f)$ must be estimated to calculate values for Q. The site response, $R(f)$, is known to be strongly dependent on local site geology, but since this study compares differences between seismograms for different events recorded at the same set of stations, variations in $R(f)$ are not important in this analysis. For the purpose of this study, $R(f)$ is assumed to be constant over the narrow observed frequency band.

The data used in this study are recorded over a relatively narrow frequency band which is generally not sufficient to independently separate source and propagation effects on the observed spectra. In order to calculate values for Q, we have assumed a simple source spectrum of the form

$$S(f) = \frac{\Omega_0}{\left(1+(f/f_0)^2\right)}, \quad f_0 = k_{p,s}\,\beta\left(\frac{16\Delta\sigma}{7M_0}\right)^{\frac{1}{3}}$$

[*Brune*, 1970; 1971] where Ω_0 is a constant proportional to the moment, f_0 is the "corner" frequency, β is the shear wave velocity at the source, $\Delta\sigma$ is the stress drop, M_0 is the moment, and $k_{p,s}$ is a constant. Brune et al. (1979) have shown that for shear waves from a wide range of source models, $k_s \approx 0.33$. For P waves, we used $k_p = 1.5\, k_s$ in accordance with observation and theoretical models [*Molnar et al.* 1973; *Madariaga*, 1976]. The stress drop for each event was assumed to be 100 bars and M_0 was estimated from the reported m_b using the M_0 - M_w relation of *Hanks and Kanamori* [1979]. For the range of magnitudes used by this study, $m_b \approx M_w$ [*Kanamori*, 1983]. For events without reported magnitudes, the magnitude was estimated from the number of reported PDE or ISC stations using the empirical relationship of *Cahill* [1990].

Average apparent Q from each event to the Jujuy network was calculated by the following procedure. Fourier amplitude spectra were calculated for both P and S waves from tapered signal windows of 2.5 and 5 s, respectively beginning at the

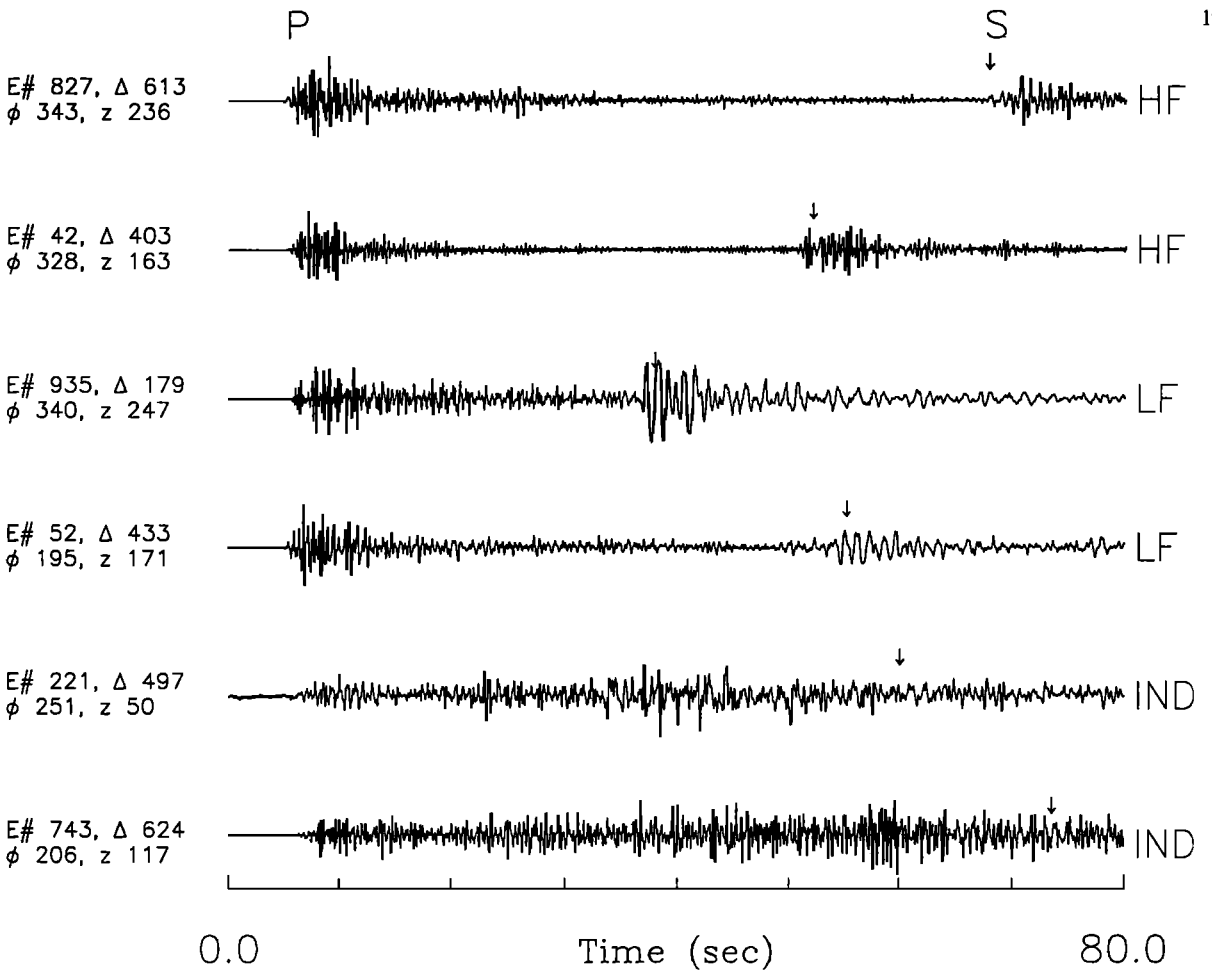

Fig. 3. Representative radial component seismograms produced by intermediate-depth events recorded at the Jujuy network showing different types of *S* waves. (HF): High-frequency *S*; (LF): Low-Frequency *S*; (IND): Indeterminant *S*. Traces are aligned at 5 s to the observed *P* wave arrival. Arrows indicate the predicted *S* arrival time. Location of events are shown in Figure 2.

onset of the phase. The spectral noise level was estimated by calculating spectra for time windows of 2.5 and 5 s immediately preceding the *P* and *S* wave onset (Figure 4). A frequency band with a signal to noise ratio exceeding 2 was selected, the average spectral noise level was subtracted from the signal spectrum, and the resulting signal was then corrected for the instrument response and source spectrum. Finally, the log spectrum was smoothed and fit to a straight line to calculate apparent Q for each event-station pair (Figure 4). An average apparent Q and standard deviation for each event to the network was then calculated from a weighted average of the estimated Q values for each event-station pair using a weighting function based on the goodness of the linear fit to each corrected spectrum.

The estimated Q values generally fall into two categories corresponding to the type (1) and (2) shear waves discussed at the end of the previous section. High-Q ray paths ($Qp > 500$, $Qs > 350$) are observed from the north and northwest of the Jujuy network, while events to the west and south of the network exhibit low values of apparent Q ($Qp < 350$, $Qs < 200$) (Figure 5). These estimated Q values are dependent on the choice of source spectral model, but as described below, we have found that over a wide range of plausible source models, the general observed pattern of Q does not significantly change, the effect of the exponential Q filter being much greater than possible variations in source spectra between events. In addition, these estimates of apparent Q are very similar to values obtained in a previous study in the region which used a source independent spectral ratio technique [*Sacks*, 1971].

We have assumed a simple source spectral model dependent on two parameters: the corner frequency, f_0, and a high-frequency decay of f^{-2}. The corner frequency used in the source spectral model, f_0, is dependent on both the estimated values for stress drop and moment. Since the corner frequency is dependent on the cube root of these values, relatively large uncertainties in these parameters result in relatively small uncertainties in the corner frequency. We have found that variations in the assumed stress drop or moment of up to 3 orders of magnitude result in variations in the estimated Q of no more than 50% Differing orientations to the focal plane can also change the corner frequency by as much as ±50% (Brune et al., 1979), but we find that the resulting estimates for Q vary by no more than ± 10%.

A larger source of error may be due to an incorrect assumption of the high-frequency rolloff above the corner frequency. We have used a source model where amplitude rolls off as f^{-2} above the corner frequency. In the model of *Brune*

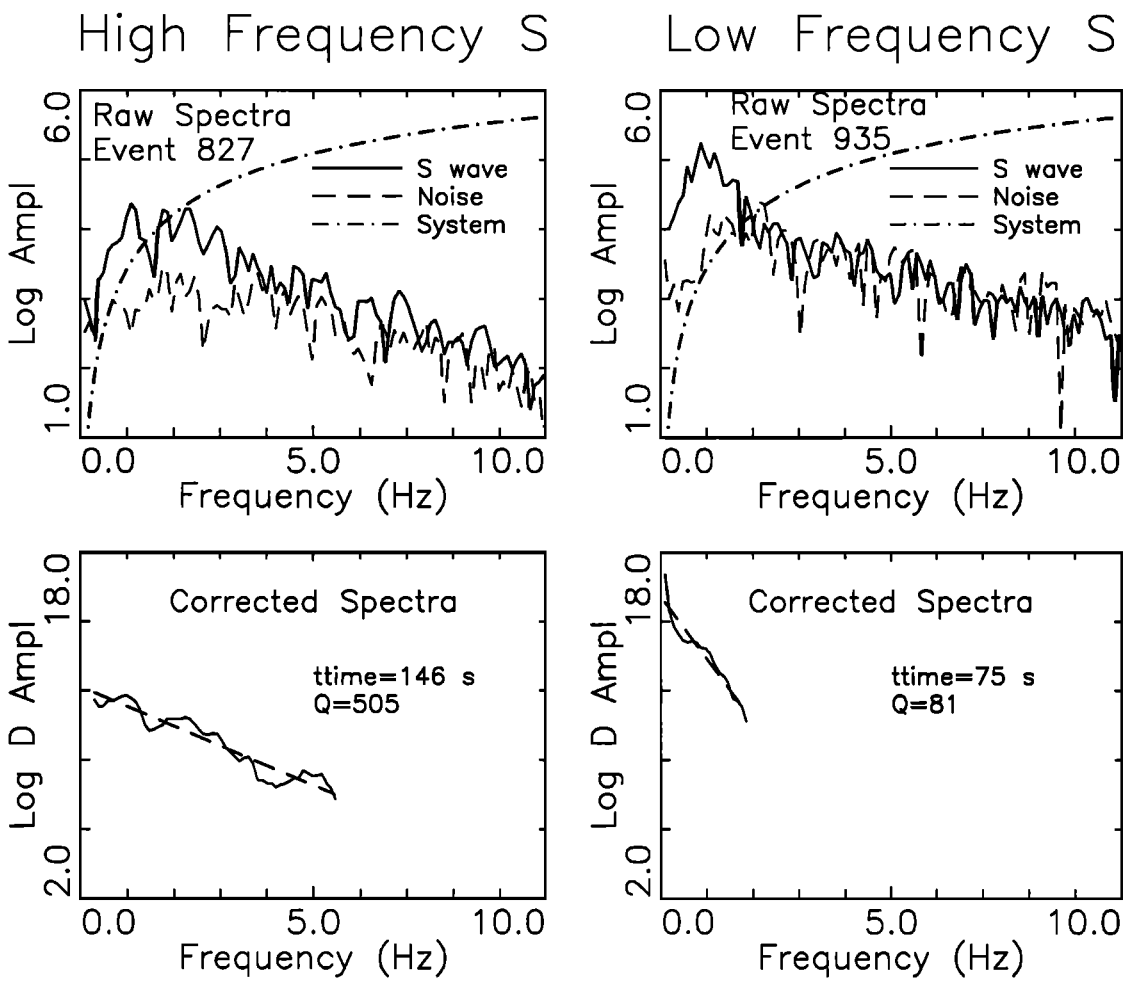

Fig. 4. (Top) Raw spectra of representative of high- and low-frequency shear waves from radial components of intermediate depth earthquakes recorded at the Jujuy array. Event numbers correspond to labeled earthquakes in Figure 2. Spectra were calculated from a tapered 5 s window beginning at the onset of the *S* wave (solid lines) and for a 5 s window immediately preceding the *S* wave (dashed lines). Also shown is the system velocity response. High-frequency *S* waves contain energy to 4 Hz, while the low-frequency *S* waves contain no energy above 2 Hz. (Bottom) Smoothed spectra corrected for source and system response (solid lines) and linear fit to the spectra (dashed lines).

[1970], the amplitude may roll off as only f^{-1} near the corner frequency for the case where the fractional stress drop is less than 1. We find that this will decrease the estimated value of Q by no more than 30%. Alternatively, a higher spectral rolloff than f^{-2}, say f^{-3}, would increase the Q estimates by a similar amount. Most of the events used in this study occur at similar depths in a similarly oriented segment of the subducted Nazca plate. Presumably, the source spectra for these events follow some type of similarity scaling law [e.g., *Aki*, 1967] over the small-magnitude range of these earthquakes. For such a case, spectral parameters such as stress drop and high-frequency decay would be the same for all events, and while the absolute values estimated for Q might be in error by as much as 50% due to uncertainties in these source spectral parameters, the relative estimates for Q between events are probably in error by less than 20% The observed relative differences between high- and low-Q seismic wave ray paths are unlikely to be due to systematic differences in the source spectra.

Errors in hypocentral locations also affect the Q estimates. However, when compared with the uncertainties due to assumptions in the source spectra, these errors are small. For a typical intermediate depth event used in this study, even a large error in hypocentral location of as much as 50 km results in a travel time error of no more than 6 s or 10% of total the travel time producing an error in Q of only around 10%.

SPATIAL PATTERN OF ATTENUATION

Mapping Lateral Changes in the Upper Mantle Structure

In this section, we present a qualitative description and interpretation of seismic wave attenuation observed at the Jujuy network, and compare these results with data observed at the Panda San Juan Argentina network and with previously reported results from WWSSN data recorded at La Paz, Bolivia. We will use these observations to map out contrasting regions of efficient and inefficient seismic wave attenuation in the upper mantle beneath the central Andean plateau. In a later section, we will present results of forward modeling of the attenuation measurements made at the Jujuy network.

The upper mantle behind volcanic arcs is often characterized by anomalously high seismic wave attenuation (low Q) and low seismic velocities and is associated with a relatively hot asthenospheric wedge situated between the upper and lower plates [e.g., *Barazangi and Isacks*, 1971; *Barazangi et al.*, 1975]. In general, the observed effects of low seismic

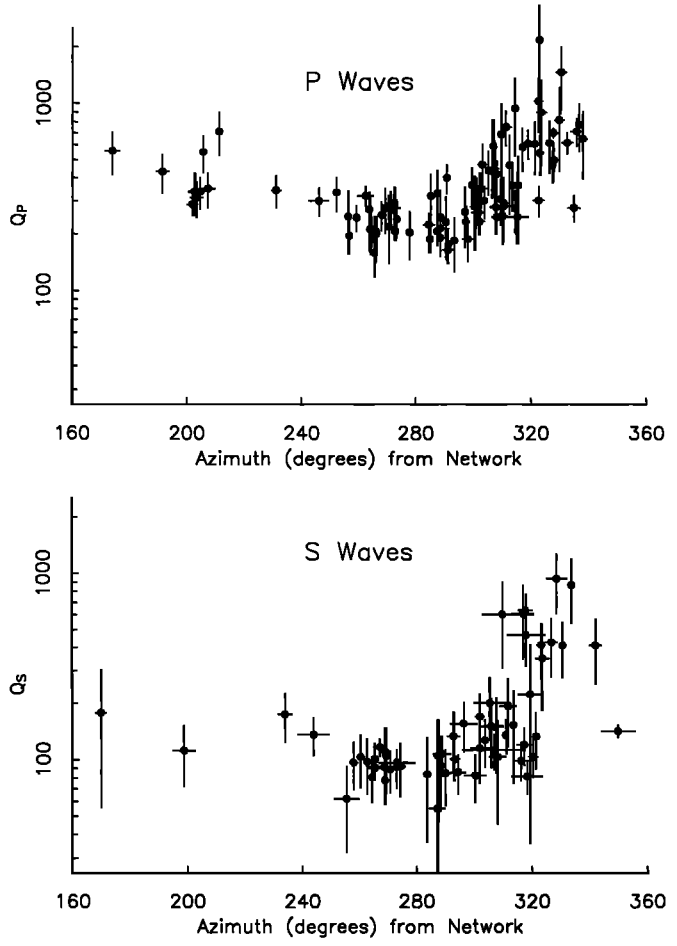

Fig. 5. Plot of the average apparent Q for each WBZ earthquake observed at the Jujuy network versus observed azimuth estimated from travel time slowness measured across the network . Vertical and horizontal error bars denote ± 1 standard deviation for each Q average and the estimated standard error of each slowness measurement , respectively.

velocities in the wedge are much more subtle than those caused by high attenuation and are difficult to observe due to hypocenteral errors and the three-dimensional complexities in the velocity structure of the subducted plate. For this reason, only the attenuation observations are used to map the structures in this study .

As an approximation, we assume that the low-Q seismic ray paths at least partially traverse the asthenospheric wedge and pass beneath regions of anomalously thinned lithosphere, whereas high-Q ray paths do not cross a significant amount of the wedge and are primarily confined to the overlying high-Q lithosphere or to the subducted Nazca plate. In addition, we assume that attenuation is primarily due to anelasticity and neglect the effect of scattering on seismic energy. Scattering can have a filtering effect on a seismic wave similar to that of anelastic attenuation with high-frequency energy scattered into the coda at the expense of the direct wave [*Richards and Menke*, 1983]. However, examination of the data indicates that the frequency content of the coda is not appreciably higher than that of the direct waves (see Figure 3). In addition, a scattering model for attenuation would predict that Q for P and S are approximately equal [*Richards and Menke*, 1983], but our estimated values of Q for P waves are considerably higher than those for S. We conclude that anelastic attenuation is the dominant mechanism affecting our data, but scattering may play an important role in the generation of the indeterminant shear waves (Figure 3).

In order to help constrain in depth the locations of regions of high and low seismic attenuation, rays were traced from the sources to the receiver array through three-dimensional (3-D) and two-dimensional (2-D) velocity models. A 3-D velocity model was constructed from a modified radially symmetric earth model, with a 90-km-thick high velocity layer corresponding to the subducted slab. Velocities in the slab were taken to be 7% higher than the surrounding mantle and the top of the subducted slab was assumed to lie 15 km above the Wadati-Benioff zone contours of *Cahill and Isacks* [1992]. 2-D velocity models were constructed at several azimuths through the 3-D model as an aid in interpretation. Rays are refracted significantly out of the plane of the 2-D models only in a few cases. We find that over a reasonably wide range of plausible velocity models, the gross ray path geometry in these models is relatively unaffected.

Observations at Jujuy, Argentina

The character and frequency content of P and S waves from Wadati-Benioff zone earthquakes vary greatly depending on the ray path to the Jujuy network. In map view high-Q ray paths are observed at Jujuy from the north and northwest while low-Q ray paths are observed from the west and south (Figures 2 and 5). Composite record sections of earthquakes at different azimuths to the network along with interpretive ray diagrams are shown in Figures 6, 7, and 8. High-frequency shear waves are observed from sources 350 to 700 km northwest of the network (events 757 and 827, Figure 6; event 42, Figure 7), whereas shear waves from sources at similar northwest azimuths but closer distances to the network exhibit a lower frequency content (event 935, Figure 6; event 80, Figure 7). Shear waves propagating from the west and southwest of the network either are low-frequency (event 769, Figure 8), or are indeterminant (event 1049, Figure 8; 743, Figure 3). The ray path geometry suggests that below around 100-km depth, a high attenuation region exists in the upper mantle beneath the plateau to the west of Jujuy, Argentina, but that a similar high attenuation region does not exist beneath the plateau north of around 22° S. This apparent along-strike change in the upper mantle attenuation structure is coincident with the boundary between the two segments of the plateau: the Altiplano and the Puna. The upper mantle beneath the Puna appears to be more highly attenuating than that beneath the Altiplano.

Indeterminant shear waves are observed from sources located near the Pacific coast of South America at depths of less than 100 km. One possible explanation for these waves is that their sources may be shallow enough to allow high-frequency P wave energy (e.g., Pg) to be channeled into the eastward thickening crust and this may obscure the later arriving shear waves. An exception to this pattern is the observation of some indeterminant shear waves from sources at around 150-km depth located beneath the eastern edge of the high Andes to the southwest of the Jujuy network (event 743, Figure 3). Perhaps scattering and multipathing due to the rapid east-west change in crustal (and presumably mantle lithospheric) structure along the propagation paths of these waves contributes to their indeterminant nature.

Seismograms from crustal earthquakes situated in the foreland fold-thrust belts to the east of the Andes differ greatly depending on azimuth to the Jujuy network. For sources

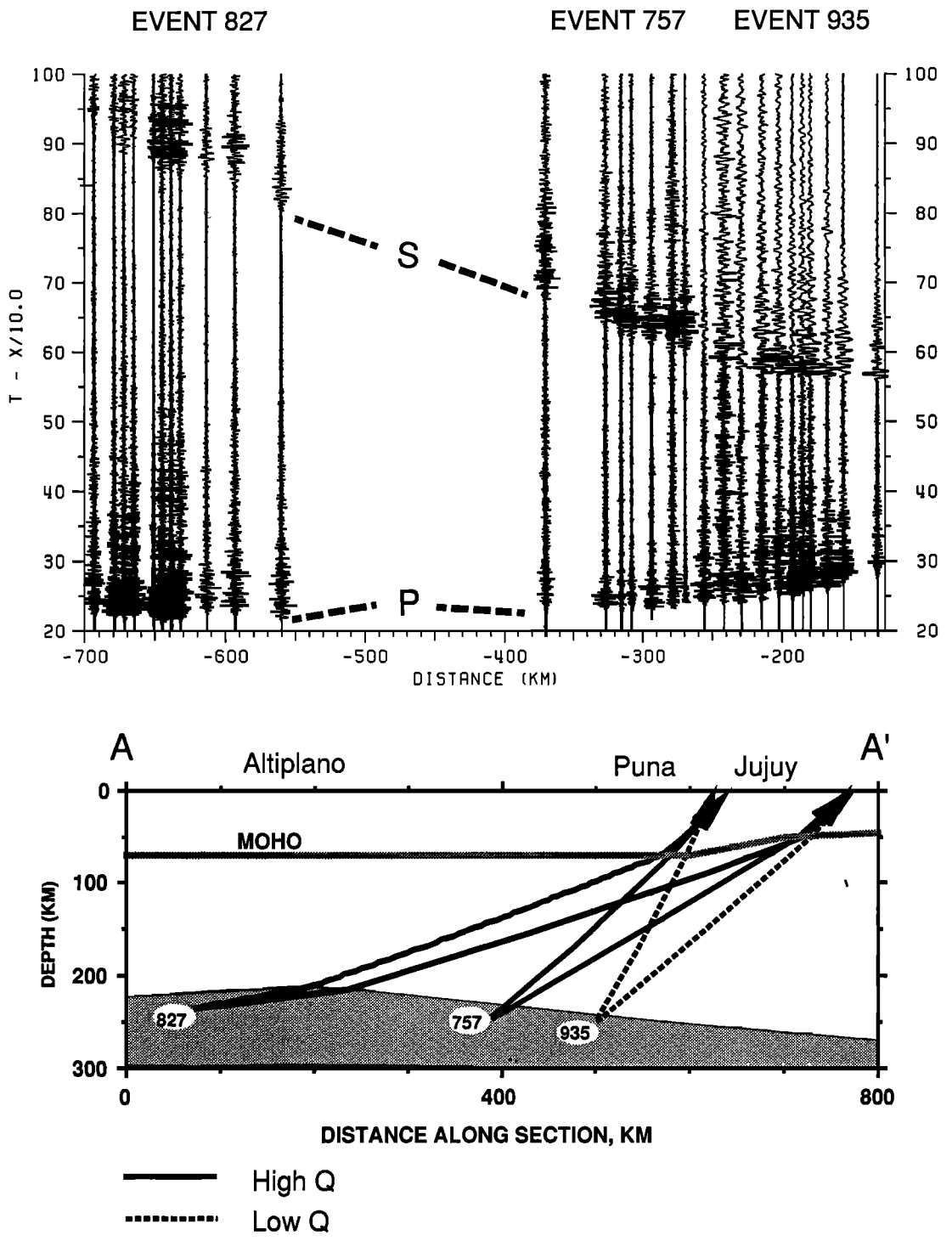

Fig. 6. Interpretive cross section and composite radial component record section constructed along line A-A' in Figure 2. Record sections are plotted at a reduction velocity of 10 km/s. Event numbers correspond to labeled earthquakes in Figure 2. Ray paths were determined from numerical ray tracing through an approximate 2-D velocity model (see text). Solid lines represent high-Q paths to the Jujuy network, while dashed lines represent low-Q paths to the Jujuy network. Section is roughly parallel to the strike of the Plateau. Event 935 contains low-frequency S waves while events 757 and 827 contain high-frequency S waves.

situated in the Subandean fold thrust belt to the north, prominent *Pn*, *Sn*, and *Lg* phases are observed in all cases, whereas for shallow events located in the Pampean ranges to the south, *Pn* is very emergent and *Sn* is not observed (Figures 2 and 9). *Pn* and *Sn* are prominent short period waves which travel through the uppermost mantle and their efficient propagation is often taken as evidence of a continuous mantle lithosphere along the propagation path [e.g., *Molnar and Oliver*, 1969]. The paths from both north and south to the Jujuy network lie entirely within the foreland thrust belts to the east of the plateau. This observation suggests that the lateral variations in the upper mantle attenuation observed beneath

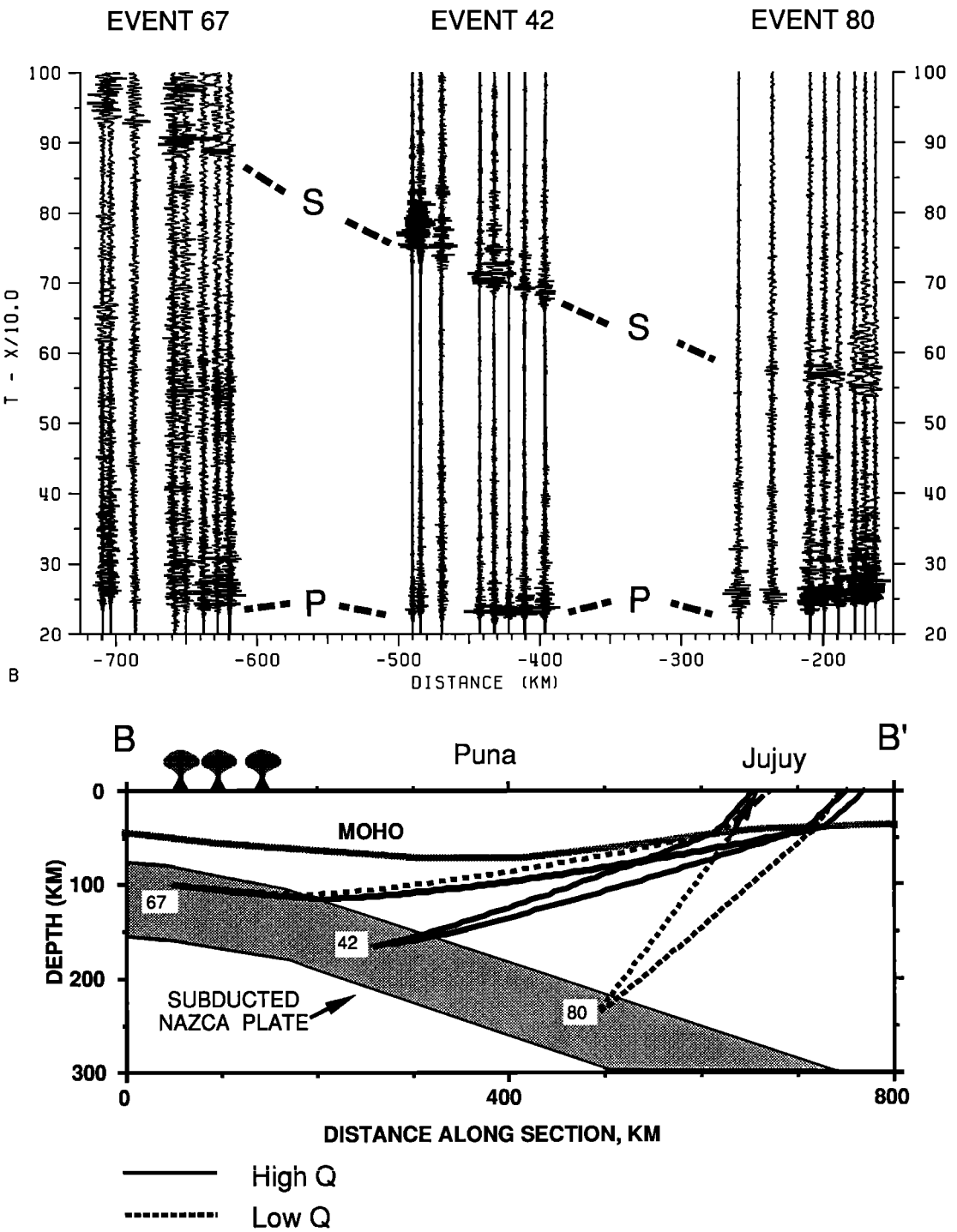

Fig. 7. Interpretive cross section and composite radial component record section constructed along line B-B' in Figure 2. Event numbers correspond to labeled earthquakes in Figure 2. Section runs oblique to the strike of the Plateau. Event 80 contains low-frequency *S* waves while event 42 contains high-frequency *S* waves. Event 67 contains both high- and low-frequency *S* wave indicating mixed paths to the array.

the plateau extend eastward beneath the Andean forelands. The absence of *Sn* from earthquakes to the south may indicate that the foreland lithosphere of the Santa Barbara ranges is thinned relative to that of the Subandean belt to the north.

Observations at San Juan, Argentina

Seismograms recorded by the San Juan network, when compared with those recorded at Jujuy from similarly located intermediate depth sources, show striking differences in frequency content (Figure 10). High-frequency shear waves (f > 5 Hz) are always observed at San Juan, while the high frequencies are often attenuated at Jujuy. The average apparent *Qs* for these paths to San Juan is 2000 or greater, while at the Jujuy network the apparent *Qs* for even the highest *Q* paths is generally less than 500. The observed differences at the two networks are partially due to differences in the crustal *Q* of the two locations, but also must be due to differences in upper

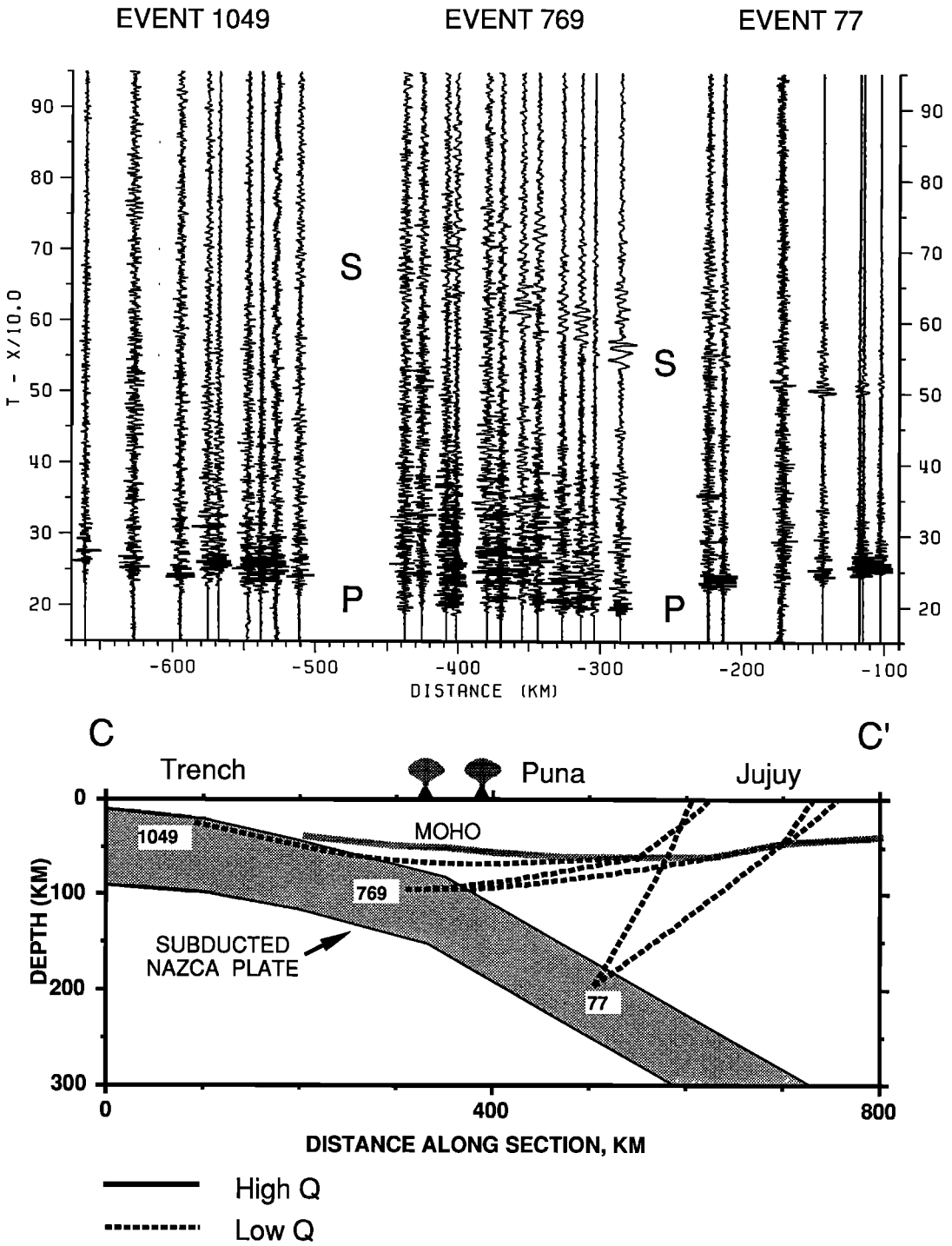

Fig. 8. Interpretive cross section and composite radial component record section constructed along line C-C' in Figure 2. Event numbers correspond to labeled earthquakes in Figure 2. Section is roughly perpendicular to the strike of the Plateau. Events77 and 769 both contain only low-frequency *S* waves. *S* waves for event 1049 are of an indeterminant nature, indicating high scattering and attenuation for the path beneath the whole width of the Andes.

mantle attenuation between the respective propagation paths to each network. Preliminary analysis of seismograms from local crustal earthquakes recorded within each of the networks indicates that Q in the uppermost crust is substantially higher beneath the San Juan network than beneath Jujuy. The higher crustal Q beneath San Juan also correlates with a greater maximum depth of seismicity [*Cahill et al.*, 1992; *Smalley et al.*, 1992]. Both these features may be a consequence of a generally warmer more ductile crust beneath Jujuy than beneath San Juan.

Differences in crustal Q cannot solely explain the high-frequency shear waves observed at San Juan. The paths to San Juan pass directly beneath the Puna and as seen at Jujuy, the asthenospheric wedge beneath the Puna efficiently attenuates the higher frequencies. It is difficult to imagine how the resulting low-frequency waves could then generate the high

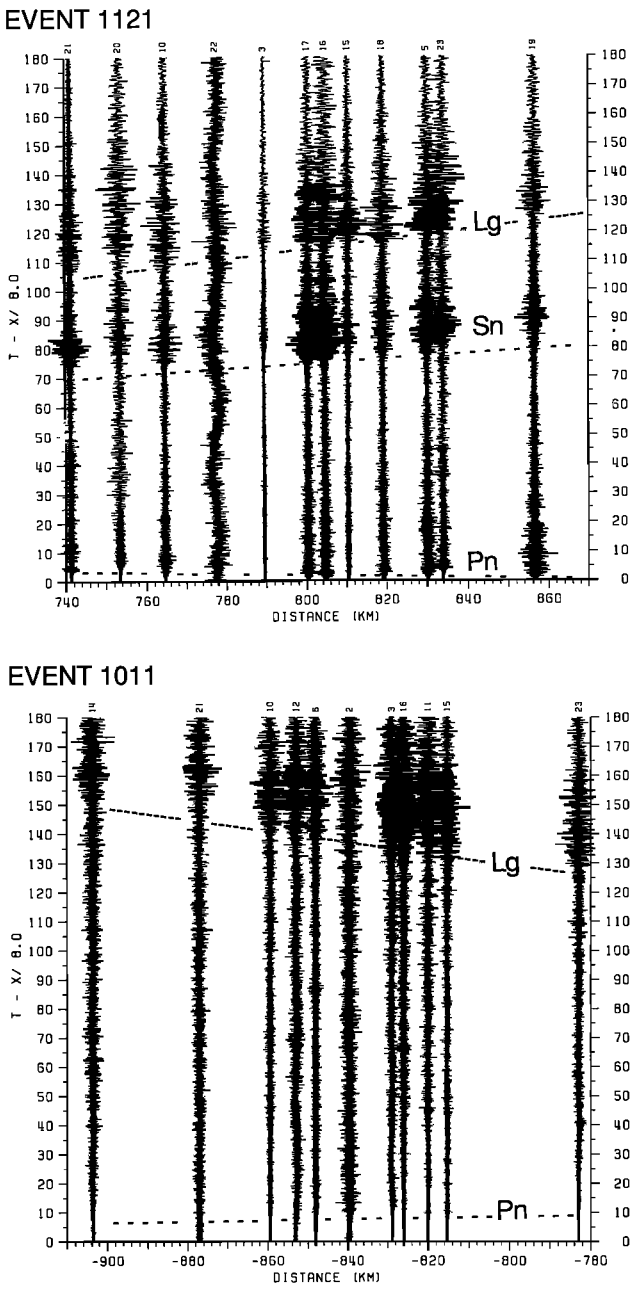

Fig. 9. Record sections containing radial components of representative shallow earthquakes located to the north (top) and south (bottom) of the Jujuy array plotted at a reduction velocity of 8 km/s. Event numbers correspond to labeled earthquakes in Figure 2. Note that *Sn* is observed for shallow events to the north but not for those located to the south.

frequencies observed at San Juan. Ray tracing indicates that for these paths to the San Juan network, rays are confined to the subducted slab as they pass beneath the Puna. The long duration and complexity of these waves suggests that they are some sort of guided wave [e.g., *Isacks and Barazangi*, 1973; *Gubbins and Snieder*, 1991]. Similar high-frequency phases have been observed at stations on the west coast of South America from intermediate depth and deep earthquakes to the east [*Sacks*, 1971; *Isacks and Barazangi*, 1973; *Chinn et al.*, 1980]. In general, these high-frequency phases are only observed at coastal stations where the subducting plate is nearly in contact with the overriding plate. Similarly, beneath San Juan the upper and lower plates are nearly in contact and a low-Q asthenospheric wedge is absent due to the shallowly dipping subduction in the region. This same explanation cannot account for the high-frequency waves observed at Jujuy, however, because while the overriding and subducting plates are nearly in contact beneath San Juan, the subducted plate lies over 250 km beneath Jujuy and 100 km or more of asthenospheric mantle wedge separates the two plates.

Ray paths for the high-frequency shear waves cross a region between 27° and 30° S where the dip of the seismic zone changes southward from 30° east to nearly horizontal and in which no intermediate depth seismicity is observed. One implication of these observations at the San Juan network is that a continuous subducted lithosphere exists across the moderate to flat dipping transition [e.g., *Bevis and Isacks*, 1984; *Cahill*, 1990; *Whitman et al.*, 1990] rather than a tear in the slab as suggested by *Barazangi and Isacks* [1976].

Observations at La Paz, Bolivia

Chinn et al. [1980] made an extensive study of shear wave propagation beneath the central Andes using WWSSN data recorded at several stations in western South America. Of particular interest are observations at La Paz, Bolivia (LPB) in the eastern Altiplano because the location of this station relative to intermediate depth earthquakes to the west is similar to that of the Jujuy network. High-frequency shear waves are observed at LPB from intermediate depth sources to the southwest while shear waves from sources at only slightly more westerly azimuths were severely attenuated (Figure 11). Ray tracing indicates that the high-frequency shear waves propagate northward for a substantial distance within the subducted slab, thus missing the highly attenuating region beneath the Puna, before leaving the slab and propagating upward to LPB (Figure 11*d*). For the more westerly azimuths (Figure 11*c*), ray paths corresponding to the highly attenuated shear waves exit the slab directly beneath the main volcanic arc. High-frequency shear waves are also observed at LPB from intermediate depth sources to the west (Figures 11*a* and 11*b*). The geometry of these ray paths is similar to that for low-Q paths observed at the Jujuy network from intermediate depth earthquakes to the west beneath the Puna (compare with event 77, Figure 8). These observations suggest that in contrast to the Puna, the Altiplano is underlain by a generally high-Q upper mantle with high attenuation (low Q) occurring only beneath the main volcanic arc.

In summary, azimuthal variations in the seismic wave attenuation observed in the eastern Andes of Argentina and Bolivia require that the upper mantle structure beneath the central Andean plateau changes along strike. Seismic ray paths to Jujuy, Argentina from sources to the west and southwest are low Q while those from more northerly azimuths are high Q. Rays to La Paz, Bolivia are low Q only for paths that leave the subducted slab beneath the main volcanic arc of the western Cordillera. Rays to San Juan are confined to the subducted slab and are not effected by the along-strike changes in the overlying mantle wedge. These observations may be combined to define a generally low-Q region in the mantle wedge beneath the plateau which varies in width along strike (Figure 12). In the Altiplano, this region is generally coincident with regions of active volcanism in the western cordillera, but beneath the Puna, the low-Q zone spans the whole width of the plateau and perhaps is present beneath the Andean foreland to the east.

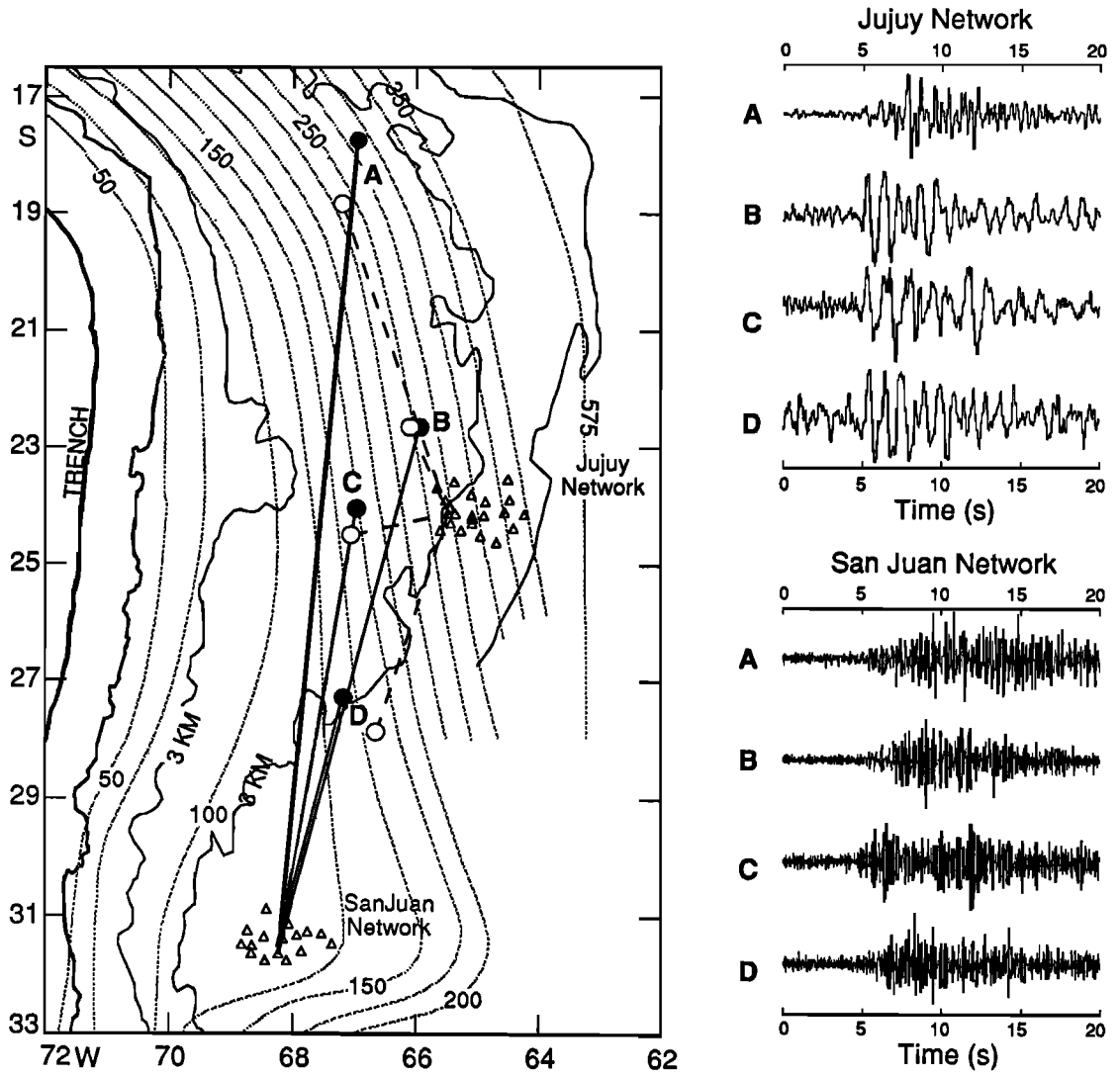

Fig. 10. Comparison of radial component shear waves from intermediate-depth earthquakes recorded at the PANDA San Juan and Jujuy networks (triangles). Events recorded at the San Juan array (solid circles) produce high-frequency shear waves which are guided along a continuous high-Q subducted lithosphere, while lower frequency shear waves are recorded at the Jujuy network.

MODELING

The results of the previous section demonstrate the need for along-strike variations in the mantle wedge beneath the central Andean plateau and adjacent foreland. The question is, where in depth do these variations take place and what are the values for Q corresponding to regions of high- and low seismic wave attenuation? The complex 3-D Q structure indicated by the previous section suggests that in order to obtain a unique and detailed image of the Q structure, attenuation measurements are required at a wide range of azimuths about the plateau. The observations reported by *Chinn et al.* [1980] are of little use in quantitatively modeling the Q structure beneath the plateau because they are based on analog World-Wide Standard Seismograph Network (WWSSN) recordings which allow only very rough Q estimates. In addition, the seismic waves recorded at the PANDA San Juan network are not useful for this purpose since their frequency content is dominated by their propagation through the subducted Nazca plate, not by the Q structure in the overlying mantle wedge. For these reasons, we are limited to the Q measurements made at the Jujuy network. Since the ray path geometry to Jujuy is not sufficient to constrain a unique Q model, we present here two extreme models in order to demonstrate the possible range of models consistent with our Q measurements.

Values for Q measured at the Jujuy network were modeled by ray tracing through the 3-D velocity model described above with lateral velocity variations confined to the subducted slab. Possible lateral variations in velocity corresponding to regions of differing seismic attenuation were ignored. Ray tracing indicates that the ray paths are not significantly affected by such subtle lateral velocity changes. For simplicity, we assume a simple three dimensional model of the subduction zone containing the following elements: (1) a high-Q subducted plate whose position is defined by the location of the Wadati-Benioff zone, (2) a variable thickness high-Q upper plate, and (3) a low-Q asthenospheric wedge between the two plates. In general, a tradeoff exists between the thickness of the low-Q zone and the Q values in the model. We therefore examined two models: (Figures 13, 14, and 15) one in which most of the seismic attenuation occurs in a relatively thick

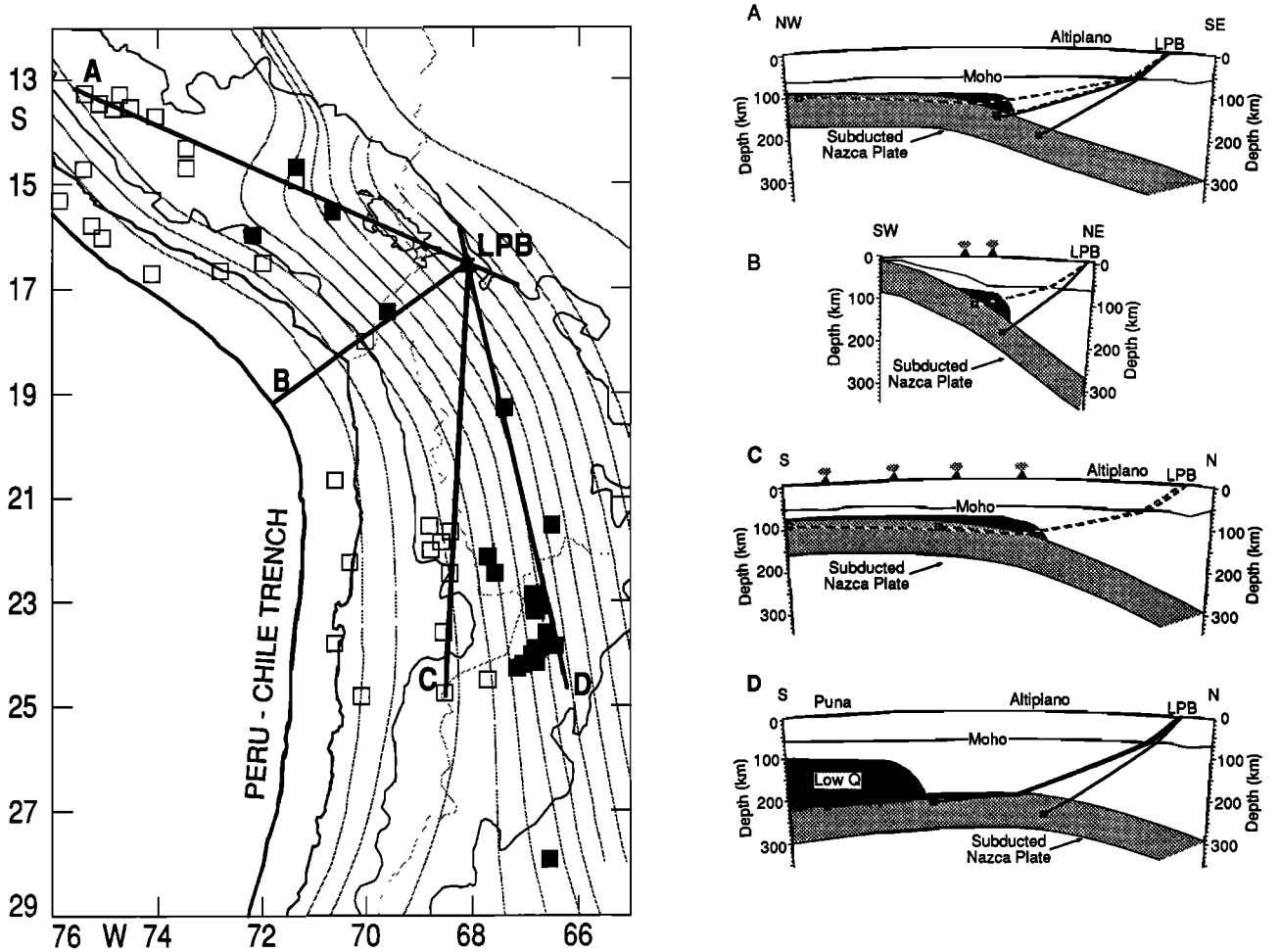

Fig. 11. (Left) Map showing location of intermediate-depth events recorded at La Paz, Bolivia (LPB) [after *Chinn et al.*, 1980]. Solid squares represent events that produced high-frequency shear waves recorded at LPB, while open squares represent events that did not produced high-frequency shear waves recorded at LPB. (Right) Interpretive ray diagrams showing cross-sectional view of high-Q paths (solid lines) and low-Q paths (dashed lines) to LPB. Shaded areas above the slab denote regions of anomalously high attenuation.

zone, and one in which the attenuation occurs in a relatively thin zone.

Model 1: variable thickness lithosphere

In the first model, model 1, we assumed that the along strike changes in attenuation were due to large along strike changes in the lithospheric thickness of the upper plate. A rough starting model of the along strike changes in lithospheric thickness was constructed based on the mapped low-Q region in the previous section. High values for Q (Qp = 4000, Qs = 2000) were assumed for the subducted plate and best fitting P and S wave Q values for the lithosphere and asthenosphere were determined by a parameter search. The shape of the overlying lithosphere was then adjusted by trial and error in order to reproduce the observed spatial pattern of attenuation. Q values for the lithosphere and asthenosphere were then readjusted in order to obtain an optimum fit to the data. Due to the larger amount of P wave data, only observations of Qp were used in adjusting the geometry of the model, but a reasonable fit was obtained for the Qs observations. In general, the modeled Q values for the asthenosphere are much better constrained than those for the lithosphere, and we find that even for models in which an infinite Q was assumed for the lithosphere, the gross geometry of the model is unchanged. The modeled Q values for the lithosphere therefore represent a lower bound. The precision of the modeling is limited by the assumptions used for the Q measurements and by the general scatter in the data. We therefore only attempted to fit the calculated values to within 30% of the observed data (Figure 16).

In model 1, most of the attenuation occurs in a low-Q asthenospheric wedge (Qp = 125, Qs = 55) which is overlain by a high-Q lithosphere (Qp = 1500, Qs = 900). The lithosphere reaches a maximum thickness of 190 km beneath the eastern Altiplano, but thins rapidly westward to a depth near the base of the crust beneath the Western Cordillera (Figures 13*a* and 14). The westward thinning of the lithosphere at this latitude is constrained by the relative location of high-Q path earthquakes beneath the central Altiplano and low-Q path earthquakes beneath the Western Cordillera (Figures 2 and 7). The intermediate depth earthquakes provide no constraint on the lithospheric thickness of the Andean foreland to the east of the Altiplano, the Subandean Ranges, but the Sn observations at Jujuy from crustal earthquakes to the north suggest that at least a "normal" thickness exists for the Subandean lithosphere to the north of Jujuy.

Farther south, beneath the Puna, the lithosphere thins to

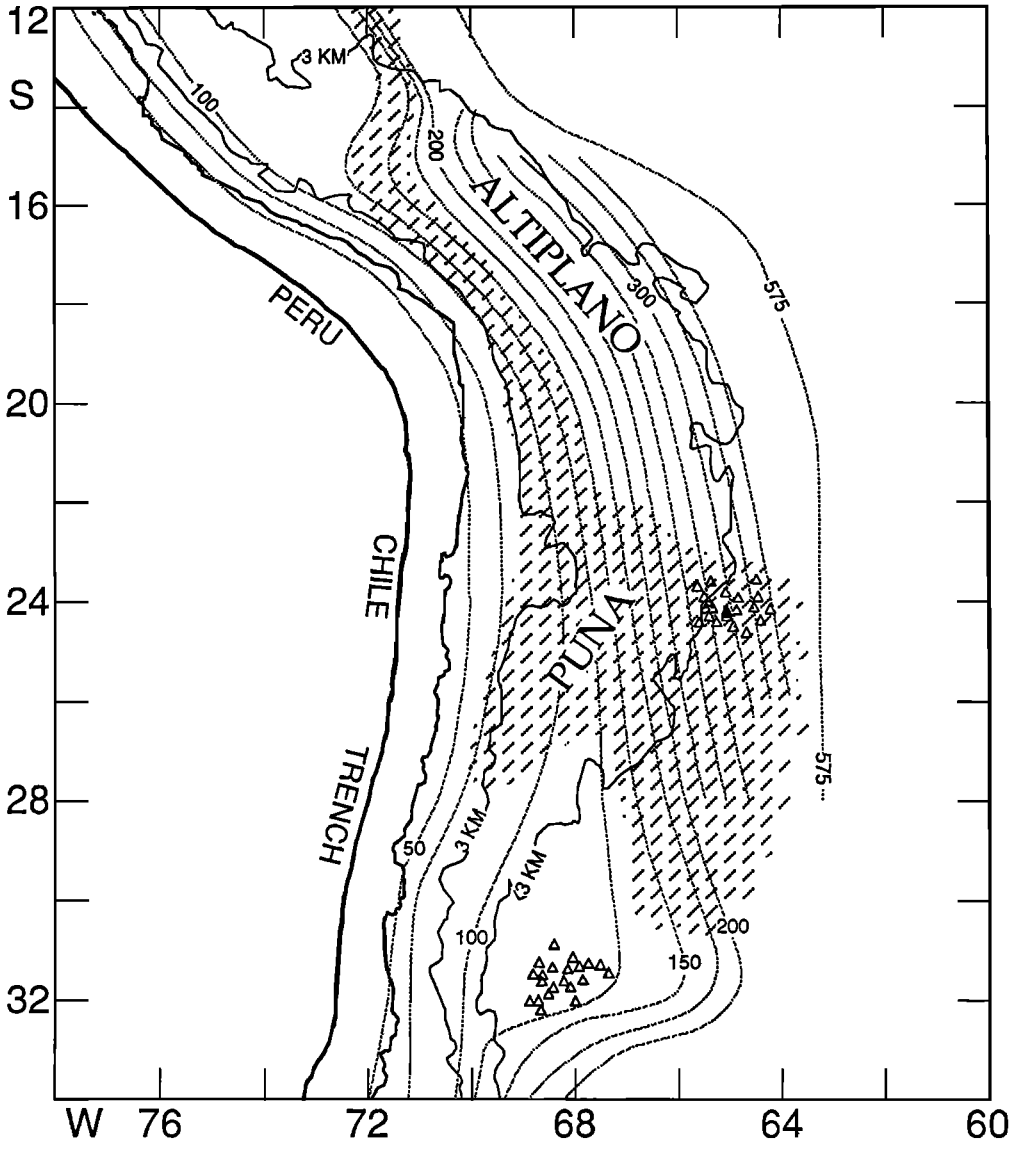

Fig. 12. Map showing regions of high seismic wave attenuation (shaded region) inferred to lie between the subducting Nazca plate and the overriding South American plate. Also shown is depth to the Wadati-Benioff zone [*Cahill and Isacks*, 1992] and the average 3-km topographic elevation contour.

near the base of the crust (60-70 km) across the whole width of the plateau before thickening to 150 km under the Andean foreland to the east (Figures 13*b* and 14). The northern boundary of the region of maximum lithospheric thinning in this model is not coincident with the physiographic boundary between the Altiplano and Puna (at around 22° S), but is instead located farther south. This southward thinning of the lithosphere across the northern Puna is constrained by observations from earthquakes situated in the Jujuy seismic nest, located 150 km west of the network (Figure 2). Q measurements from nest events are generally low, with Q subtly decreasing from north to south (see Figure 5). In addition, the nest is oriented oblique to the general strike of the Wadati-Benioff zone such that the depths of earthquakes in the nest increase to the northwest, and rays from events in the northern part of the nest must traverse a thicker section of mantle than for earthquakes farther to the south. This required increasing the thickness of the lithosphere from south to north across the nest such that rays from all the nest events traverse a similar thickness of asthenosphere. The extreme thinning of the lithosphere to the base of the crust in the central Puna is required not by earthquakes from the Jujuy nest, but by earthquakes situated to the west beneath the main volcanic arc. Rays from these earthquakes must propagate for a substantial distance within the asthenosphere to produce the low-Q observations, and since the raypaths from these earthquakes are generally confined to depths shallower than 100 km (see Figure 8, event 769 for an example), the lithosphere must be very thin along these paths. Alternatively, if our assumption of constant Q within the asthenosphere is relaxed and we allow lower Q material in the asthenosphere beneath the main volcanic arc than beneath the plateau, the lithosphere beneath the central Puna need only be thinned to perhaps 90 km.

To the south of the Puna, the lithosphere again thickens to 100 km in the northern Pampean ranges and the extreme thinning of the lithosphere modeled beneath the Puna does not extend to the east of the plateau. The thickness of the lithosphere beneath the northern Pampean ranges is

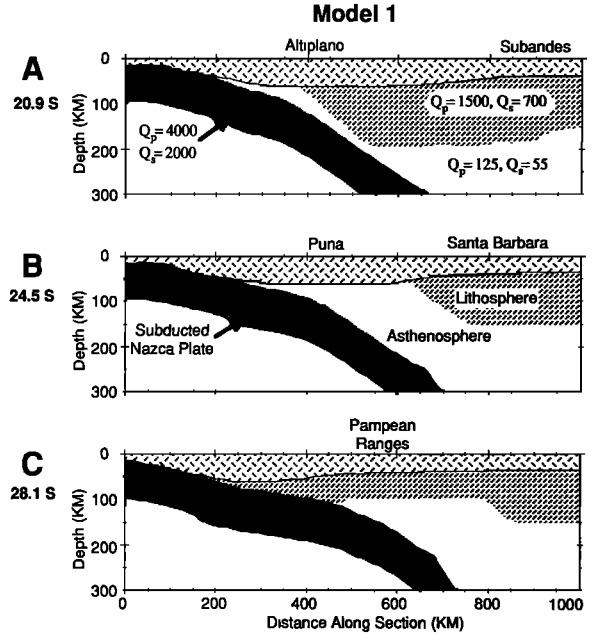

Fig. 13. E-W cross sections through three-dimensional Q model 1. For model 1, azimuthal variations in observed seismic attenuation at Jujuy are assumed to be due to changes in thickness of a high-Q lithosphere. Location of sections is shown in Figure 14.

constrained by earthquakes to the southwest of the Jujuy network which occur at depths between 115 and 180 km. The highest measured Q values are observed from the shallowest and most westerly of these earthquakes (Figure 2, event 743) and rays from these events spend much more of their paths in the lithosphere than the deeper, lower Q events to the east. The relatively thin lithosphere modeled for the Andean foreland to the south of Jujuy is consistent with the absence of Sn observed at Jujuy from crustal earthquakes to the south.

Model 2: thin low-Q zone above the subducted slab

In an alternative model, model 2, we assumed that the observed spatial pattern of attenuation was due to the presence or absence of a relatively thin (25 km) low-Q layer situated immediately above the subducted plate (Figure 15). The values for Q and the shape of this layer were then adjusted in manner similar to model 1. Q in the upper layer was constrained to be near the average measured Q for the high-Q ray paths from the northwest of Jujuy. The modeled Q values for the upper layer (Qp = 700, Qs = 400) represent the average for the asthenosphere and lithosphere along the high-Q ray paths, whereas the thin low-Q layer represents lateral heterogeneity within the asthenospheric wedge. In map view, the low-Q zone generally corresponds to the low-Q region qualitatively mapped in the previous section (Figure 12). At the latitude of the Altiplano, the low-Q zone is present only beneath the western cordillera whereas beneath the Puna, the zone spans the whole width of the plateau. To the southeast of the Puna, the low-Q zone is localized beneath the northern Pampean ranges but does not extend farther west than 67° W longitude.

The modeled Q values for the low-Q zone (Qp = 30, Qs = 11) are indicative of substantial proportions of melt [*Sato et al.*, 1989] and in general, the low-Q region spatially corresponds to regions of active volcanism. This would suggest a genetic relationship between the low-Q zone, partial melt in the asthenosphere and the occurrence of active volcanism beneath the western cordillera and beneath the whole width of the Puna. An exception to this pattern is the low-Q zone beneath the northern Pampean ranges which does not lie below a region of recent volcanism. The lithospheric thinning model, model 1, might be more appropriate for this region and would also better explain the poor Sn propagation northward to Jujuy.

Discussion and Conclusions

The primary result of this study is that the upper mantle structure of the central Andean plateau cannot be described by a simple 2-D model. The lithospheric thickness of the upper plate and/or the asthenospheric structure of the mantle wedge must change from north to south. We have investigated two simplified upper mantle models to explain our observed spatial pattern of seismic attenuation. In model 1, the pattern of attenuation is explained by thinning the lithosphere by an extreme amount beneath the center of the plateau, from 180 km beneath the Altiplano to 70 km beneath the Puna. In an alternative model, the lateral changes in seismic attenuation are caused by variable width, 25 km thick, extremely low-Q zone in the asthenosphere beneath the plateau. The thin low-Q zone of model 2 is similar to that proposed by *Sacks and Okada* [1974] for northern Chile (~ 24° S). Clearly, however, this thin layer does not extend beneath the whole width of the plateau farther north.

The two models are not incompatible with each other, because a thick lithosphere might impede circulation in the underlying asthenospheric wedge resulting in lower temperatures and higher Q values. Alternatively, a hotter more well developed asthenospheric wedge might promote increased stoping and thermal thinning of the overlying lithosphere. We favor a hybrid of the two models with along-strike variations in both the lithospheric thickness and thermal properties of the asthenospheric wedge. Hopefully in the future, additional data will allow further refinement of this model.

The along-strike segmentation in upper mantle structure is coincident with changes in the topography, physiography and tectonic style of the plateau, and with the foreland structures to the east of the plateau. Several converging lines of evidence suggest that these along-strike changes at the surface might also be due to changes in lithospheric thickness (e.g., model 1). The Puna is on average at a higher elevation than the Altiplano [see *Isacks*, 1988, plate 1] and this is consistent with an increased amount of thermal uplift due to the thinned Puna lithosphere. This model suggests that the two segments of the plateau are supported by different modes of isostatic compensation with thermal expansion (lithospheric thinning) playing a greater role relative to crustal thickening in producing plateau uplift for the Puna than for the Altiplano. The along-strike changes in tectonic style of both the plateau and its adjacent foreland to the east might also be a consequence of a change from thick lithosphere beneath the Altiplano and Subandean ranges to a thinner and rheologically weaker lithosphere beneath the Puna and Santa Barbara system. The weaker lithosphere of the Puna-Santa Barbara segment has led to a greater degree of basement involved deformation than for the thin-skinned structures to the north.

In many ways, the tectonic style of the Puna segment is similar to the thick-skinned tectonics of the Pampean ranges farther south. Pampean type structures extend well north of the

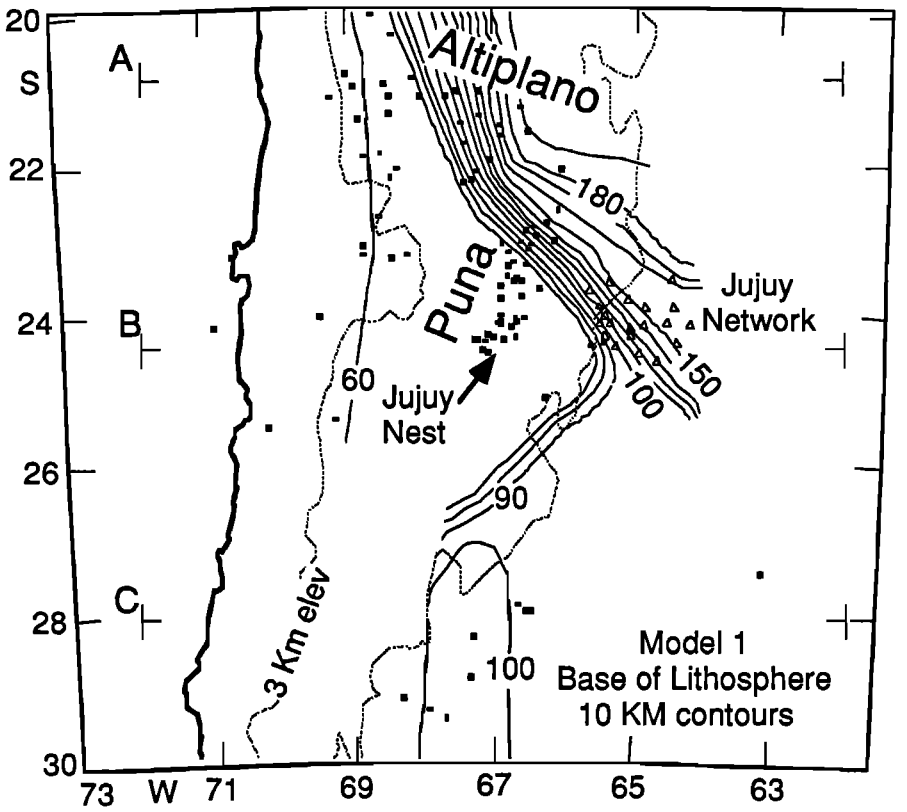

Fig. 14. Map showing contours to base of high-Q lithosphere in model 1, location of intermediate depth earthquakes used in this study (small squares), and PANDA Jujuy network (triangles). Contours interval is 10 km. Contours are not shown in unconstrained regions of the model. Location of cross sections in Figures 13 and 15 are also shown.

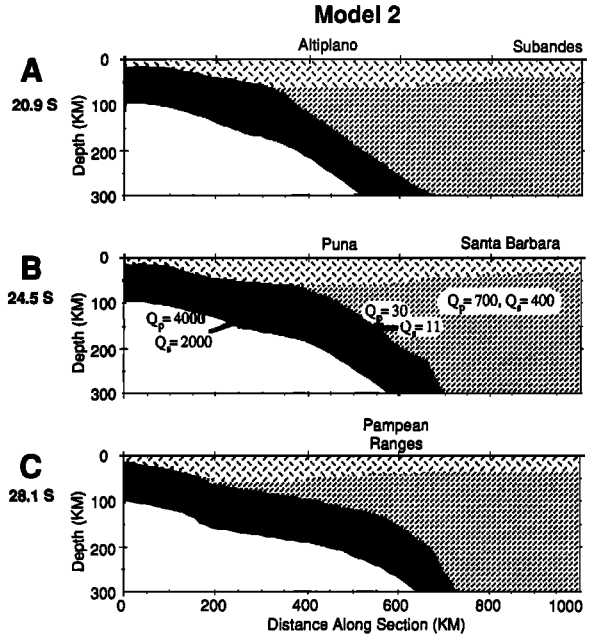

Fig. 15. E-W cross sections through three dimentional Q model 2. For model 2, azimuthal variations in observed seismic attenuation at Jujuy are assumed to be due to the existence of a thin low-Q zone above the slab (dark shaded pattern). Location of sections is shown in Figure 14.

region of flat subduction into the southern Puna and its adjacent foreland thrust belt [*Allmendinger et al.*, 1989; *Strecker et al.*, 1989]. The thickness of the upper plate beneath the Pampean ranges near San Juan, Argentina is tightly constrained to be less than 90-100 km from seismicity studies of the underlying Wadati-Benioff zone [*Smalley and Isacks*, 1987] and this lithospheric thickness is comparable to that inferred for the Puna from this study (Figure 13). The similarities in tectonic style may have arisen from similarities in lithospheric thickness and the consequent overall rheology of the plate. The lower average elevation of the Pampean segment is a consequence of the horizontally subducted Nazca plate located directly beneath the upper plate with little or no intervening asthenospheric wedge [e.g., *Smalley and Isacks*, 1990].

The southward increase in upper mantle seismic attenuation beneath the plateau is also coincident with changes in the distribution of Neogene arc and backarc volcanic rocks. On the western edge of the plateau, the region of high seismic attenuation is roughly coincident with the Altiplano Puna volcanic complex, a region of extensive ignimbrite volcanism erupted since ~10.4 Ma which is thought to be the result of large-scale crustal melting [*de Silva*, 1989]. One possible heat source for this large-scale crustal melting is the inflow of hot asthenospheric material beneath the thinned Puna lithosphere. A similar relationship is observed for recent mafic backarc volcanics erupted on the plateau. Young back-arc lavas in the Altiplano and the northern Puna are predominantly shoshonitic in composition and small in volume indicating sources with relatively small melt percentages. To the south, back-arc volcanics progressively increase in volume and change in composition from shoshonitic to calc-alkaline to OIB (oceanic island basalt) type and this suggests a progressive increase in percentage of melt and a decrease in lithospheric contamination from north to south [*Knox et al.*, 1989, *Kay et al.*, 1990; *Coira and Kay*, 1992, *Kay and Kay*, 1992). Again, these observations are consistent with our lithospheric thinning model.

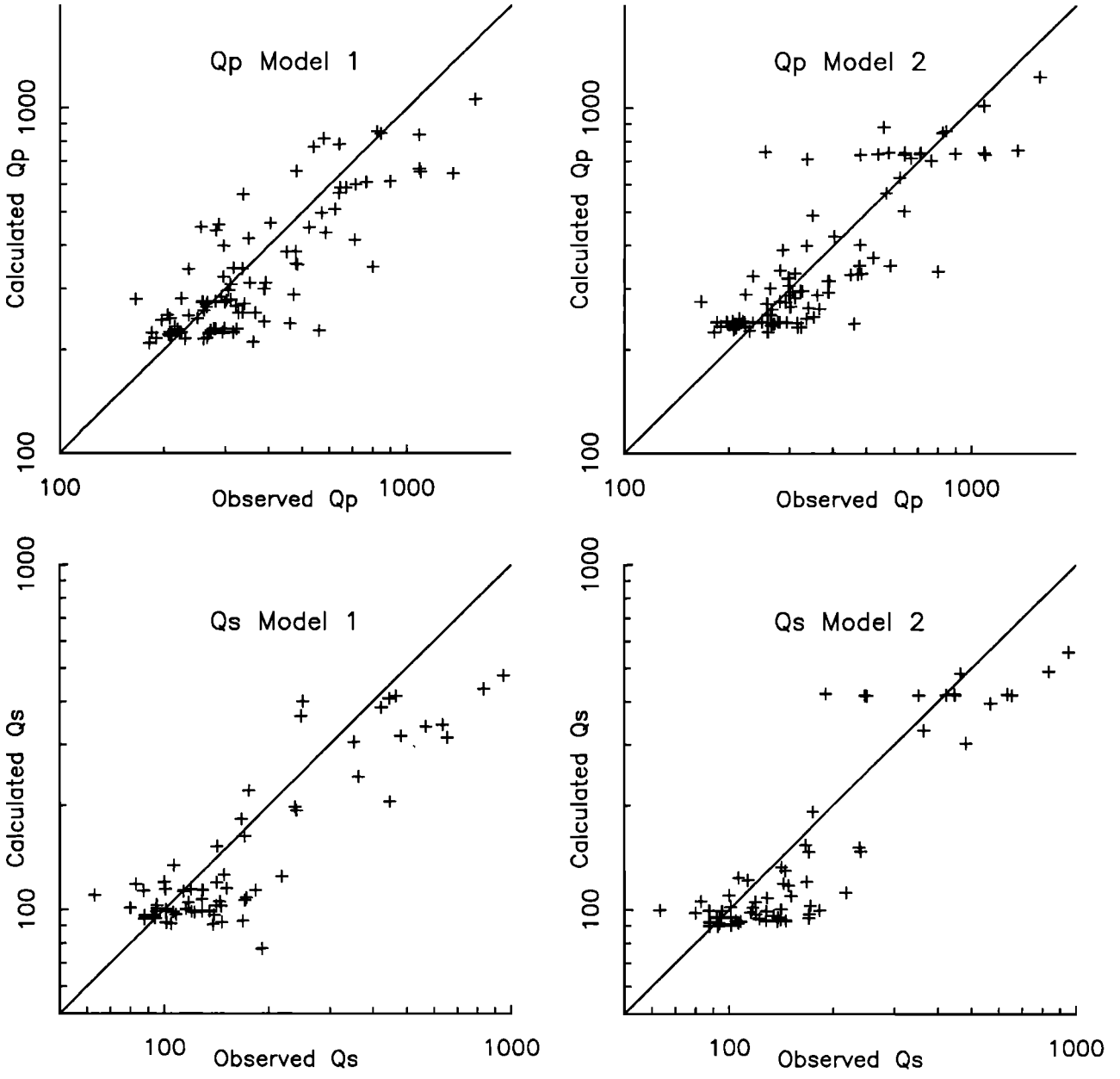

Fig. 16 . Scatter plot comparing average observed Q for each event and the calculated average event Q for models 1 and 2. The calculated values generally fall within 30% of the observations.

We have proposed that the along-strike segmentation of the central Andean plateau and its adjacent foreland fold-thrust belts is caused by a southward decrease in lithospheric thickness near 22° S. The mechanism responsible for this change is unclear and several possibilities exist. Perhaps the change in lithospheric thickness predates the main stage of Andean uplift, or that preexisting lithospheric properties of the two segments have at least influenced a later change in the thickness. It is unclear how the lateral segmentation of the plateau correlates with postulated late Proterozoic-early Paleozoic terrane boundaries in the region [*Ramos*, 1988], but differences in the foreland structures of the two segments have existed as far back as the Paleozoic [*Allmendinger et al.*, 1983]

Alternatively, this change in lithospheric thickness might be due to a larger amount of shortening across the mountain belt in the north with the underthrust Brazilian shield accounting for the thick lithosphere beneath the Altiplano. This model implies that the Altiplano has been translated towards the foreland relative to the Puna and requires as much as 200 km or more shortening for the Altiplano segment than for the Puna (see Figures 13*a* and 13*b*). Clear evidence is lacking, however for a large scale shear zone or strike-slip fault between the Altiplano and the Puna. Perhaps the change in shortening is gradual.

Finally, the lateral change in lithospheric thickness might be due to a relatively recent removal of lithosphere beneath the Puna. Possibly, this is related to the progressive southward flattening of the subducted Nazca plate over the past 18 m.y. [*Kay et al.*, 1988], with the stoping and removal of lithosphere caused by advective corner flow in the asthenospheric wedge above the steep to flat transition. Data from earlier regional wave propagation studies [*Sacks*, 1971; *Chinn et al.*, 1980] suggest that a similar high attenuation zone may exist near the transition from steep to flat subduction beneath southern Peru

(also see Figure 12). Alternatively, the removal of lithospheric material may have been even more recent. At around 2 Ma, the regional stress system in the Puna reoriented, from predominantly thrust to strike-slip fault kinematics [*Allmendinger*, 1986; *Marrett*, 1989, 1990], and this may be due to a gravitationally driven delamination of the mantle lithosphere and possibly lowermost crust of the Puna [Kay et. al., 1990; Kay and Kay; 1992].

Acknowledgments. The PANDA Jujuy seismic experiment was a collaborative effort involving personnel from CERI-MSU, Cornell University, ORSTOM, and the Instituto de Minería y Geología in Jujuy. The authors wish to thank members of the technical field crew in Jujuy: James Bollwerk, Francis Bondoux and Klaus Bataille. Robert Smalley and Gregory Steiner developed software and hardware, respectively, for the PANDA network. We are grateful to Betty Coira and Waldo Chayle of the Instituto de Minería y Geología for valuable consultations regarding the geology of Jujuy province. We thank Rick Allmendinger, Muawia Barazangi, Terry Jordan, Sue Kay, and others in the Cornell Andes project for helpful discussions and guidance in the tectonic interpretation of the data. Muawia Barazangi , Mark Woods, and an anonymous referee provided helpful critical reviews of the manuscript. This study was supported by NSF grants EAR-8804976, EAR-9005222, and EAR-9118201.

REFERENCES

Aki, K.,Scaling law of seismic spectrum, *J. Geophys. Res.*, *72*, 1217-1231, 1967.

Allmendinger, R. W., Tectonic development, southeastern border of the Puna Plateau, northwestern Argentine Andes, *Geol. Soc. Am. Bull.*,*97*, 1070-1082, 1986.

Allmendinger, R. W., V. A. Ramos, T. E. Jordan, M. Palma, and B. L. Isacks, Paleogeography and Andean structural geometry, northwest Argentina, *Tectonics*, *2*, 1-16, 1983.

Allmendinger, R. W., M. Strecker, J. E. Eremchuk, and P. Francis, Neotectonic deformation of the southern Puna Plateau, Northwestern Argentina, *J. S. A.Earth Sci.*, *2*, 111-130, 1989.

Baby, P., G. Herail, J. M. Lopez, O. Lopez, J. Oller, J. Pareja, T. Sempere, and D. Tufiño, Structure de la Zone Subandine de Bolivie: influence de la géométrie des séries sédimentaires antéorogéniques sur la propagation des chevauchements,*Tectonique*, *309*, 1717-1722, 1989.

Baker, M.C.W., The nature and distribution of upper Cenozoic ignimbrite centres in the central Andes, *J. Volcanol. Geotherm. Res.*, *11*, 293-315, 1981.

Barazangi, M., and B.L. Isacks, Lateral variations of seismic wave attenuation in the upper mantle above the inclined earthquake zone of the Tonga island arc: Deep anomaly in the upper mantle, *J. Geophys. Res.*, *76*, 8493-8516, 1971.

Barazangi, M., and B. L. Isacks, Spatial distribution of earthquakes and subduction of the Nazca Plate beneath South America, *Geology*, *4*, 686-692, 1976.

Barazangi, M. , W. Pennington, and B.L. Isacks, Global study of seismic wave attenuation in the upper mantle behind island arcs using pP waves, *J. Geophys. Res.*, *80*, 1079-1092, 1975.

Bevis, M., and B. L. Isacks, Hypocenteral trend surface analysis: probing the geometry of Benioff zones, *J. Geophys. Res.*, *89*, 6153-6170, 1984.

Brune, J. N., Tectonic stress and the spectra of seismic shear waves from earthquake sources, *J. Geophys. Res.*, *75*, 4997-5009, 1970.

Brune, J. N., Correction, *J. Geophys. Res.*, *76*, 5002, 1971.

Brune, J. N., R. J. Archuleta, and S. Hartzell, Far-field S-wave spectra, corner frequencies, and pulse shapes, *J. Geophys. Res.*, *84*, 2262-2272, 1979.

Cahill, T., Earthquakes and tectonics of the central Andean subduction zone,Ph.D. thesis, 225 pp., Cornell University, Ithaca, N.Y., 1990.

Cahill, T., and B. L. Isacks, Seismicity and shape of the subducted Nazca plate, *J. Geophys. Res.*, in press, 1992.

Cahill, T., B. L. Isacks, D. Whitman, J.-L. Chatelain, A. Perez, and J.M. Chiu, Seismicity and tectonics in Jujuy Province, northwest Argentina, *Tectonics*, in press, 1992.

Chinn, D. S., B. Isacks, and M. Barazangi, High-frequency seismic wave propagation in western South America along the continental margin, in the Nazca plate and across the Altiplano. *Geophys. J. R. Astron. Soc.*, *60*, 209-244, 1980.

Chiu, J.M., G.C. Steiner, R. Smalley, Jr., and A.C. Johnston, The PANDA seismic array -A simple, working system, *Bull. Seismo. Soc. Am.*, *81*, 1000-1014, 1991.

Coira, B., and S. M. Kay, Implications of Quaternary volcanism at Cerro Tuzgle for crustal and mantle evolution of the high-Puna plateau, central Andes, Argentina, *Contrib.Mineral.Petrol.*, in press, 1992.

de Silva, S. L., Altiplano-Puna volcanic complex of the central Andes, *Geology*, *17*, 1102-1106, 1989.

Dewey, J. F., and J. Bird, Mountain belts and the new global tectonics, *J. Geophys. Res.*, *75*, 2625-2647, 1970.

Fielding, E. J., Neotectonics of the central andean cordillera from satellite imagery, Ph.D. thesis, 213 pp., Cornell University, Ithaca, N.Y, 1989.

Froidevaux, C., and B. L. Isacks, The mechanical state of the lithosphere in the Altiplano-Puna segment of the Andes, *Earth Planet. Sci. Lett.*, *71*, 305-314, 1984.

Grier, M. E., The influence of the Cretaceous Salta rift basin on the development of Andean structural geometries, NW Argentine Andes, Ph.D. thesis, Cornell University, Ithaca, N.Y, 1990

Gubbins, D., and R. Snieder, Dispersion of P waves in the subducted lithosphere: Evidence for an eclogite layer, *J. Geophys.. Res.*, *96*, 6321-6333, 1991.

Hanks, T. C. and H. Kanamori, A moment magmitude scale, *J. Geophys. Res.*, *84*, 2348-2350, 1979.

Isacks, B. L., Uplift of the central Andean plateau and bending of the Bolivian orocline, *J. Geophys. Res.*, *93*, 3211-3231, 1988.

Isacks, B. L., and M. Barazangi, High frequency shear waves guided by a continuous lithosphere decending beneath western South America, *Geophys. J. R. Astron. Soc.*, *33*, 129-139, 1973.

James, D. E., Andean crustal and upper mantle structure, *J. Geophys. Res.*, *76*, 3246-3271, 1971*a*.

James, D. E., Plate tectonic model for the evolution of the central andes, *Geol. Soc. Am. Bull*, *82*, 3325-3346, 1971*b*.

Jordan, T. E., and R. N. Alonso, Cenozoic stratigraphy and basin tectonics of the Andes Mountains, 20°-28° south latitude, *Am. Assoc. Pet. Geol. Bull.*,*71*, 49-64, 1987.

Jordan, T. E., B. L. Isacks, R. W. Allmendinger, J. A. Brewer, V. A. Ramos, and C. J. Ando, Andean tectonics related to geometry of subducted Nazca plate, *Geol. Soc. Am. Bull.*, *94*, 341-361, 1983.

Kanamori, H., Magnitude scale and quantification of earthquakes, *Tectonophysics*, *93*, 185-199, 1983.

Kay, R. W., and S. M. Kay, Delamination and delamination magmatism,*Tectonophysics*, in press, 1992.

Kay, S. M., V. Maksaev, R. Moscoso, C. Mpodozis, C. Nasi, and C. E. Gordillo, Tertiary Andean magmatism in Chile and Argentina between 28° S and 33° S: Correlation of magmatic chemistry with a changing Benioff zone, *J. S. Am. Earth Sci.*, *1*, 21-38, 1988.

Kay, S. M., B. Coira, and J. Viramonte, Basalt to high-Mg andesite chemistry as a guide to the mantle and the significance of a seismic gap in the southern Argentine Puna of the central Andes (abstract), *E Trans. AGU*, *71*, 1719, 1990.

Knox, W. J., S. M. Kay, and B. Coira, Geochemical evidince for the origin of Quaternary basaltic sndesites of the Puna, Northwest Argentina, *Rev. Asoc. Geol. Argentina*, *64*, 194-206, 1989.

Lyon-Caen, H., P. Molnar, and G. Suárez, Gravity anomalies and flexure of the Brazilian Shield beneath the Bolivian Andes, *Earth and Planet. Sci. Let.*, *75*, 81-92, 1985.

Madariaga, R., Dynamics of an expanding circular fault, *Bull. Seismol. Soc. Am.*, *66*, 639-666, 1976.

Marrett, R.A., The Late Cenozoic tectonic evolution of the Puna plateau and adjacent foreland, northwestern Argentina, Ph.D. thesis, 365 pp., Cornell University, Ithaca, N.Y., 1990

Marrett, R.A., R. Allmendinger, and M. Grier, Kinematic changes during Late Cenozoic deformation of the southern Puna plateau: Argentine Andes, 23°S-27°S latitude: *28th Symposium International Geologic Congress*, *2*, 372-373,1989.

Mingramm, A., A. Russo, A. Pozzo, and L. Casau, Sierras subandinas, in *Segundo Simposio de Geología Regional Argentina*, pp. 95-138, Academía Nacional de Ciencias, Córdoba, 1979.

Molnar, P. and J. Oliver, Lateral variations of attenuation in the upper mantle and discontinuities in the lithosphere, *J. Geophys. Res.*, *74*, 2648-2682, 1969.

Molnar, P., B. E. Tucker, and J. N. Brune, Corner frequencies of P and S waves and models of earthquake sources, *Bull. Seismol. Soc. Am.*, *63*, 2091-2105, 1973.

Pilger, R. H., Jr., Plate reconstructions, aseismic ridges, and low-angle subduction beneath the Andes, *Geol. Soc. Am. Bull.*, *92*, 448-456, 1981.

Ramos, V. A., Late Proterozoic-early Paleozoic of South America A collisional history, *Episodes, 11*, 168-174, 1988.

Richards, P. G., and W. Menke, The apparent attenuation of a scattering medium, *Bull. Seismol. Soc. Am., 73*, 1005-1021, 1983.

Roeder, D., Andean-age structure of Eastern Cordillera (Province of La Paz, Bolivia), *Tectonics*, *7*, 23-39, 1988.

Sacks, I. S., The Q-structure of South America, *Year Book,Carnegie Inst. Wash.,70*, 340-343, 1971.

Sacks, I. S., and H. Okada, A comparison of the anelasticity structure beneath western South America and Japan, *Phys. Earth Planet. Inter.*, *9* , 211-219, 1974.

Sato, H., I. S. Sacks, T. Murase, G. Muncill, and H. Fukuyama, *Qp*-melting temperature relation in peridotite at high pressure and temperature: attenuation mechanism and implications for the mechanical properties of the upper mantle, *J. Geophys. Res., 94*, 10,647-10,661, 1989.

Sheffels, B. M., Lower bound on the amount of crustal shortening in the central Bolivian Andes, *Geology, 18*, 812-815, 1990.

Smalley, R. F., Jr., and B. L. Isacks, A high resolution local network study of the Nazca Plate Wadati-Benioff zone under western Argentina, *J. Geophys. Res., 92*, 13,903-13,912, 1987.

Smalley, R. F., Jr., and B. L. Isacks, Seismotectonics of thin and thick-skinned deformation in the Andean foreland From local network data: Evidence for a seismogenic lower crust, *J. Geophys. Res., 95*, 12,487-12,498, 1990.

Smalley, R. F., Jr., J. Pujol, M. Regnier, J.-M. Chiu, J.-L. Chatelain, B. L. Isacks, M. Araujo, and N. Puebla, Basement seismicity beneath the Andean Precordillera thin-skinned thrust belt and implications for crustal and lithospheric behavior, *Tectonics*, in press, 1992.

Strecker, M. R., P. Cerveny, A. L. Bloom, and D. Malizia, Late Cenozoic tectonism and landscape development in the Foreland of the Andes: Northern Sierras Pampeanas (26° - 28° S), Argentina, *Tectonics, 8*, 517-534, 1989.

Thorpe, R. S., P. W. Francis, and R. S. Harmon, Andean andesites and crustal growth, *Philos. Trans. R. Soc. London., 301*, 305-320, 1981.

Whitman, D., T. Cahill, B. Isacks, J. L. Chatelain, A. Perez, and J. M. Chiu, High frequency wave propagation in the subducted Nazca Plate, western South America (abstract), *E Trans. AGU ,71*, 1462, 1990.

J.-L. Chatelain, Office de la Recherche Scientifique et Technique Outre-Mer (ORSTOM), IRIGM-LGIT, Universite J. Fourier, BP 53X, 38041 Grenoble Cedex, France.

J.-M Chiu, Center for Earthquake Research and Information, Memphis State University, 3904 Central Avenue, Memphis, Tennessee 38152.

B. L. Isacks, and D. Whitman, Institute for the Study of the Continents (INSTOC) and Department of Geological Sciences, Cornell University, Ithaca, New York 14853.

A.Perez, Instituto de Minería y Geología, Universidad Nacionál de Jujuy, 5400 San Salvador de Jujuy, Argentina.

(Received September 9, 1991;
revised July 16, 1992;
accepted July 20, 1992.)